

ANNUAL SUMMARY

Atlantic Hurricane Season of 2001

JOHN L. BEVEN II, STACY R. STEWART, MILES B. LAWRENCE, LIXION A. AVILA, JAMES L. FRANKLIN, AND
RICHARD J. PASCH

NOAA/NWS/Tropical Prediction Center/National Hurricane Center, Miami, Florida

(Manuscript received 19 July 2002, in final form 9 December 2002)

ABSTRACT

Activity during the 2001 hurricane season was similar to that of the 2000 season. Fifteen tropical storms developed, with nine becoming hurricanes and four major hurricanes. Two tropical depressions failed to become tropical storms. Similarities to the 2000 season include overall activity much above climatological levels and most of the cyclones occurring over the open Atlantic north of 25°N. The overall “lateness” of the season was notable, with 11 named storms, including all the hurricanes, forming after 1 September. There were no hurricane landfalls in the United States for the second year in a row. However, the season’s tropical cyclones were responsible for 93 deaths, including 41 from Tropical Storm Allison in the United States, and 48 from Hurricanes Iris and Michelle in the Caribbean.

1. Overview of the 2001 season

The National Hurricane Center (NHC) tracked 15 tropical cyclones (TCs) that achieved tropical storm or hurricane strength in the Atlantic basin during 2001 (Table 1). Nine of these became hurricanes and four became “major hurricanes” [category 3 or higher on the Saffir–Simpson hurricane scale (SSHS) (Simpson 1974) with maximum 1-min-average winds greater than 96 kt (1 kt = 0.514 m s⁻¹)]. These numbers were higher than the climatological average of 10 named storms, six hurricanes, and two major hurricanes and were comparable to the 15 tropical and subtropical storms, eight hurricanes, and three major hurricanes of 2000 (Franklin et al. 2000). Additionally, there were two tropical depressions that failed to reach tropical storm strength.

As in 2000, most of the 2001 activity occurred over the subtropical regions north of 25°N. Six named storms formed in this region from nontropical weather systems, and several cyclones that formed in the deep Tropics reached peak intensity in this region. Indeed, there were no hurricanes in the area south of 23°N and east of 70°W. Five cyclones in the deep Tropics dissipated, although four of them (Chantal, Dean, Erin, and Felix) later reformed. Four cyclones (Allison, Karen, Noel, and Olga) were subtropical cyclones during a portion of their life

cycle—simultaneously exhibiting characteristics of both tropical and extratropical cyclones (Hebert 1973).

No hurricanes struck the United States during 2001. The season thus joins the 2000, 1990, and 1951 seasons as years in which eight or more hurricanes occurred without a U.S. hurricane landfall. Additionally, the 2000–01 period was the first time since the 1981–82 seasons that the United States experienced consecutive seasons without a landfalling hurricane. However, Tropical Storms Barry and Gabrielle were just under hurricane strength at landfall in Florida.

Another aspect of the 2001 season was its relative “lateness.” Eleven storms, including all hurricanes, formed after 1 September, and the last storm (Olga) dissipated on 4 December, after the official end of the season. Only the 1887 and 1969 seasons produced more TCs during the September–November period. The first hurricane (Erin) did not form until 8 September, the latest such occurrence since 1984. The last major hurricane (Michelle) reached peak intensity on 3–4 November, thus becoming the second major hurricane to occur in November in the past 3 years.

Atlantic TCs directly caused 93 deaths in 2001. Iris and Michelle were category-4 hurricanes in the northwestern Caribbean that killed 31 and 17 people, respectively. Tropical Storm Allison was the deadliest and most destructive cyclone, causing 41 deaths and damage exceeding \$5 billion in the southern and eastern United States. This was the deadliest and costliest *tropical storm* in U.S. history.

Corresponding author address: Dr. John L. Beven II, National Hurricane Center, 11691 SW 17th St., Miami, FL 33165-2149.
E-mail: John.L.Beven@noaa.gov

TABLE 1. Atlantic tropical storms and hurricanes of 2001.

Name	Class*	Dates**	Max 1-min wind speed (kt)	Min sea level pressure (mb)	Deaths	U.S. damage (\$ million)
Allison	T	5–17 Jun	50	1000	41	5000+
Barry	T	2–7 Aug	60	990	2	30
Chantal	T	14–22 Aug	60	997	0	0
Dean	T	22–28 Aug	60	994	0	2
Erin	H	1–15 Sep	105	968	0	0
Felix	H	7–18 Sep	100	965	0	0
Gabrielle	H	11–19 Sep	70	975	2	230
Humberto	H	21–27 Sep	90	970	0	0
Iris	H	4–9 Oct	125	948	31	0
Jerry	T	6–8 Oct	45	1005	0	0
Karen	H	12–15 Oct	70	982	0	0
Lorenzo	T	27–31 Oct	35	1007	0	0
Michelle	H	29 Oct–5 Nov	120	933	17	0.1
Noel	H	4–6 Nov	65	986	0	0
Olga	H	24 Nov–4 Dec	80	973	0	0

* T—tropical storm, maximum sustained winds 34–63 kt; H—hurricane, maximum sustained winds 64 kt or higher.

** Dates based on UTC time and include tropical depression stage.

Section 2 describes the individual tropical storms and hurricanes of 2001 along with data sources used in analyzing and tracking them. Tropical depressions and other weather systems are discussed in section 3. Section 4 presents a discussion on the verification of NHC official forecasts, and section 5 provides a concluding discussion.

2. Tropical storm and hurricane summaries

Individual cyclone summaries are based on “best track” data resulting from the NHC’s poststorm meteorological analyses of all available observations. The best track consists of 6-hourly center locations, maximum sustained (1-min average) surface (10 m) wind, and minimum sea level pressure. The life cycle of the cyclone includes the tropical (or subtropical) depression stage. That evolution, and portions of the extratropical stage, are shown in Fig. 1.

A vital (and often sole) source of information is imagery from geostationary meteorological satellites—the American *Geostationary Operational Environmental Satellites* (GOES)-8 and -10 and the European *Meteorological Satellite*-7. The imagery is interpreted using the Dvorak (1984) technique for TCs and the Hebert–Poteat (1975) technique for subtropical cyclones. These intensity estimates are provided by the Tropical Analysis and Forecast Branch (TAFB) of the Tropical Prediction Center, the Satellite Analysis Branch of the National Environmental Satellite, Data, and Information Service (NESDIS), and the Air Force Weather Agency. Geostationary satellite data are also the source for wind vectors derived through the methodology of Nieman et al. (1997)

Geostationary data are supplemented with that from other satellites. The most frequently used data are multichannel microwave imagery (Hawkins et al. 2001) from the Defense Meteorological Satellite Program po-

lar-orbiting satellites and the National Aeronautics and Space Administration’s (NASA) Tropical Rainfall Measuring Mission. These data provide detailed information on TC convective structure and aid in determining center locations. Additionally, the Advanced Microwave Sounding Unit on the National Oceanic and Atmospheric Administration’s (NOAA) polar-orbiting satellites provides information on thermal structure (Brueske et al. 2002). Other supplemental satellite information includes oceanic surface wind data from the NASA SeaWiFS instrument on the Quick Scatterometer (QuikSCAT) satellite (Tsai et al. 2000). These data can define the TC wind field and help determine whether a tropical disturbance has a closed surface circulation.

In situ data for systems posing a threat to land are generally available from aircraft reconnaissance flights conducted by the Hurricane Hunters of the 53d Weather Reconnaissance Squadron of the Air Force Reserve Command and the NOAA Aircraft Operations Center. During these flights, minimum central pressures are either measured by dropsondes released at the circulation center or extrapolated hydrostatically from flight-level measurements. Surface or near-surface winds in the eyewall or maximum wind band are often measured directly using global positioning system (GPS) dropwindsondes (Hock and Franklin 1999), but are also frequently estimated from flight-level winds through empirical relationships derived from the GPS dropwindsondes (Franklin et al. 2000). During important forecast situations, regular reconnaissance flights may be complemented by “synoptic surveillance” missions by NOAA’s G-IV jet aircraft, which releases dropwindsondes over oceanic areas to fill data voids (Aberson and Franklin 1999). Aircraft reconnaissance during 2001 was significantly augmented by the NOAA–NASA Hurricanes at Landfall/Fourth Convection and Moisture Experiment (CAMEX-4), which sampled Chantal, Erin,

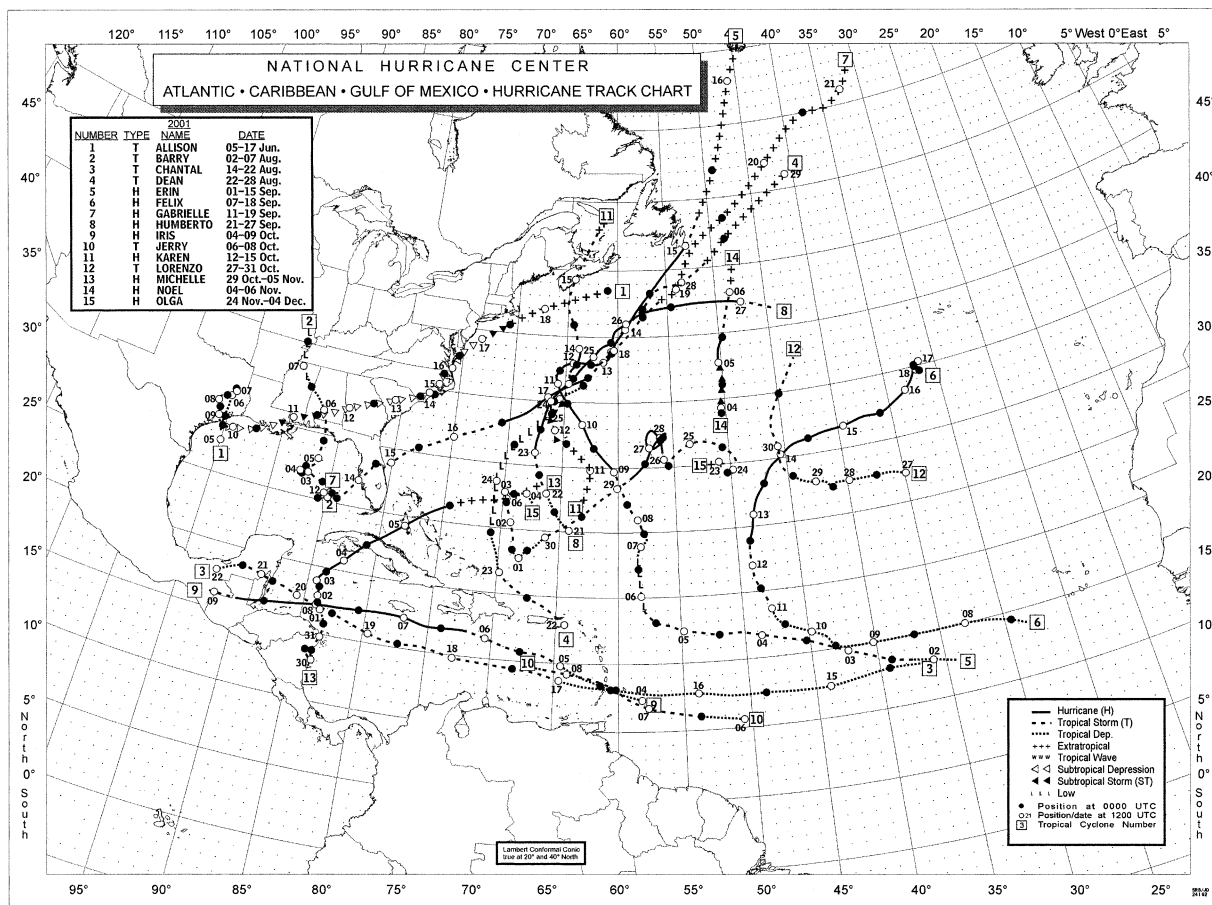


FIG. 1. Atlantic tropical storms and hurricanes of 2001.

Gabrielle, and Humberto, and by a research flight into Karen by Environment Canada.

Other data sources include observations from land stations, upper-air stations, radars, ships, and buoys. The 2001 season saw notable contributions of surface observations from nonstandard sources. Mesoscale data networks run by universities and non-NOAA government institutions provided poststorm data from Allison, Barry, and Gabrielle, while the general public provided important observations of Barry.

a. Tropical Storm Allison

Allison formed near the upper Texas coast and meandered over southeastern Texas, producing torrential rainfall and catastrophic floods in the Houston area. Allison then acquired subtropical cyclone characteristics and produced heavy rains and floods near its track from Louisiana eastward to North Carolina, and then northward along the U.S. east coast to Massachusetts.

1) SYNOPTIC HISTORY

Allison originated from a tropical wave that crossed the west coast of Africa on 21 May. Little development

occurred as the wave moved westward to northern South America by 26 May, the southwestern Caribbean Sea by 29 May, and the extreme eastern North Pacific Ocean by 1 June. A low- to midlevel cyclonic circulation that formed about 200 n mi south-southeast of Salina Cruz, Mexico, on 2 June moved inland over southeastern Mexico and western Guatemala the next day. The low-level circulation weakened after landfall, while the midlevel circulation moved over the southern Yucatan Peninsula early on 4 June.

The midlevel circulation moved northwestward into the Bay of Campeche by early 5 June. Aided by diffluent produced by an upper-level low over southern Texas, convection developed on the cyclonic-shear side of a low-level jet extending from Yucatan to the Texas-Louisiana border. By 1200 UTC, satellite imagery and surface observations suggested a surface circulation had formed about 120 n mi south of Galveston, Texas. A strong pressure gradient east of the center helped produce a large area of tropical storm force winds at that time, so the best track of Allison starts as a tropical storm (Fig. 1). However, Allison did not exhibit a classical tropical appearance because of the nearby upper-level cold low.

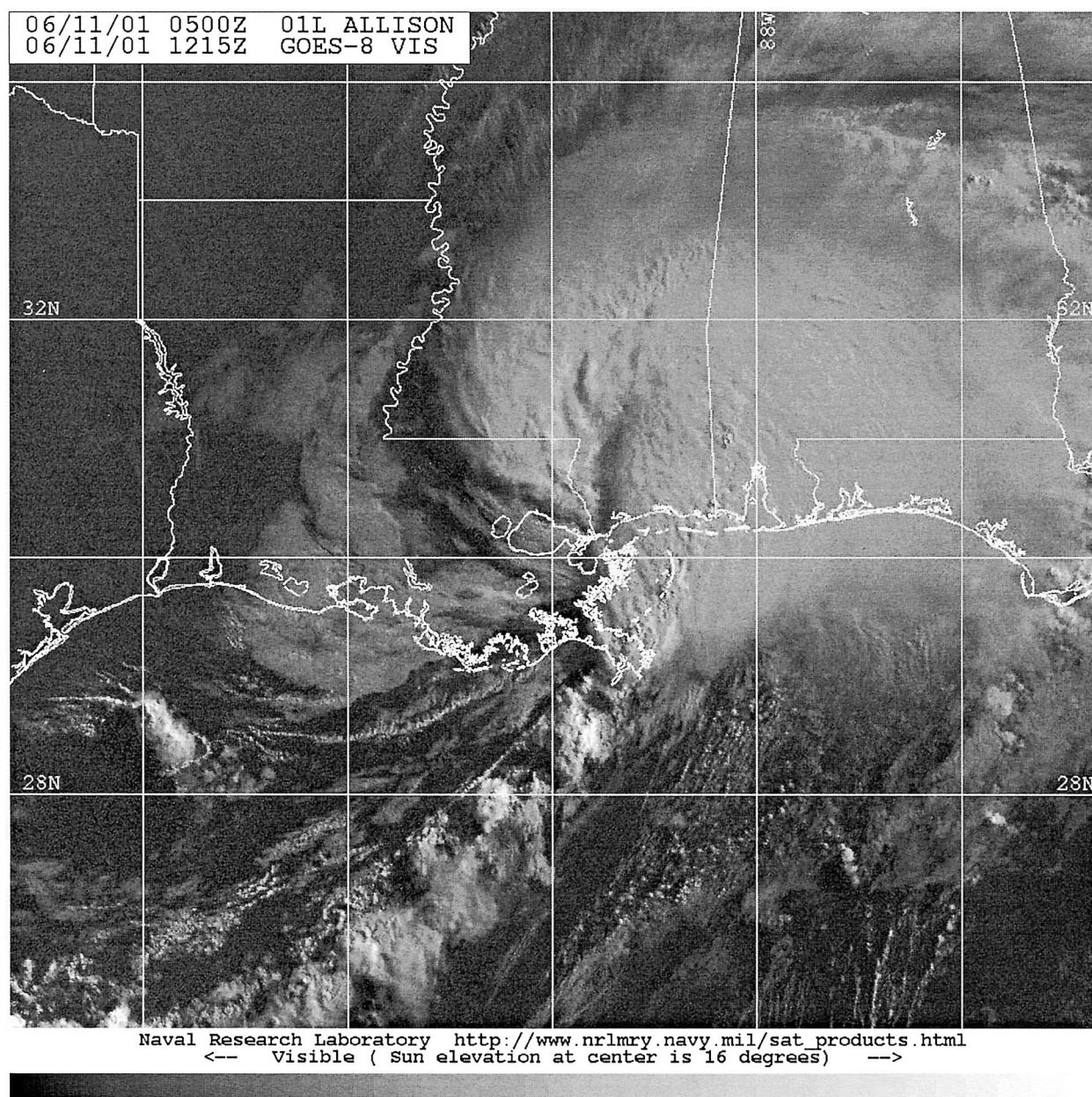


FIG. 2. GOES-8 visible image of Allison as a subtropical storm at 1215 UTC 11 Jun 2001. Image provided by the Naval Research Laboratory's Marine Meteorology Division in Monterey, CA.

Allison reached its peak intensity of 50 kt at 1800 UTC 5 June. Slight weakening occurred before landfall near Freeport, Texas, 3 h later. Allison then weakened to a depression as the center passed just west of Houston early on 6 June. It became stationary near Lufkin, Texas, on 7 June.

Allison drifted southward on 8 June, and eventually emerged over the Gulf of Mexico near Freeport early on 10 June. An upper-level trough interacted with Allison as it reached the Gulf, with the upper-level temperature gradient causing the cyclone to acquire sub-

tropical characteristics. Vertical wind shear forced convection well to the east of the center, with a new center forming near the convection early on 11 June. The new center moved east-northeastward and made landfall as a subtropical depression near Morgan City, Louisiana, around 0200 UTC that day.

After the second landfall, convection became better organized and surface reports indicated that Allison became a subtropical storm by 0600 UTC. Radar data showed the formation of an "eyelike" feature near 1200 UTC (Fig. 2). However, surface data indicated light

TABLE 2. (Continued)

Location	Min sea level pressure		Max surface wind speed			Storm surge (m) ^c	Storm tide (m) ^d	Total rain (mm)
	Time (UTC)/date	Pressure (mb)	Time (UTC) ^a /date	Sus-tained (kt) ^b	Gust (kt)			
Buffalo Bayou								597.9
Chigger Creek (Windsong)								477.0
Clear Creek (Telephone Rd.)								509.0
Conroe								459.2
Conroe (KCXO)	0757 6 Jun	1002.7	0444 6 Jun		26			444.0
Deer Park								584.0
Coward Creek (at Baker)								709.9
Dickinson								367.8
Eagle Point (port)	0230 6 Jun	1005.4	2130 5 Jun	37	42			
Ellington Field (KEFD)	0250 6 Jun	1004.4	0130 6 Jun	20	44			
Freeport								307.8
Friendswood								659.9
Furr High School (Harris County)								892.6
Galveston (KGLS)	0215 6 Jun	1004.4	2123 5 Jun	33	40			248.1
Galveston Bay, N Jetty	0012 6 Jun	1002.9	2116 5 Jun	35	42	0.5		
Galveston Bay, S Jetty	0100 6 Jun	1003.4	2106 5 Jun	34	47			
Galveston Pleasure Pier	0130 6 Jun	1003.7	2118 5 Jun	38	45	0.6		
Garners Bayou								625.1
Grant								543.8
Greens Bayou								908.3
Harris County Museum of Natural Science								529.1
Heights								812.8
Houston Hobby (KHOU)	0253 5 Jun	1004.4	2254 5 Jun	27	33			476.8
Houston Intercontinental (KIAH)	0413 6 Jun	1003.0	0313 6 Jun	21	28			418.6
Hunting Bayou (Houston)								908.1
Huntsville (KUTS)	0943 6 Jun	1003.7						308.9
Imperial Sugar								395.5
Jamaica Beach	0100 6 Jun	1004.3						308.1
Kingwood								533.4
La Porte								479.0
Lawndale								545.1
League City WFO	0300 6 Jun	1005.6	2100 5 Jun		25			493.0
Little Vince (at Jackson)								569.0
Missouri City								278.9
Morgans Point (port)	0300 6 Jun	1004.6	0318 6 Jun	27	36	0.4		
Palacios (KPSX)	0048 6 Jun	1005.8	0003 6 Jun		24			
Pearland (KLVJ)	0300 6 Jun	1004.1	2216 5 Jun	26	32			543.8
Pennington								396.2
Port of Houston								939.5
Sabine Pass						0.8		
Stella Link								500.9
Sugarland (KSGR)	0336 6 Jun	1005.4	2225 5 Jun		25			244.1
Sugarland City Hall								388.9
Tomball								411.5
Tomball (KDWH)	0559 6 Jun	1003.4	0409 6 Jun	21	29			333.8
Vince Bayou (W. Ellaine)								642.9
Westheimer (Houston)								838.2
Westbury								496.1
White Oak Bayou (Ella)								462.0
Winnie								421.1
C-MAN stations								
Cape Lookout, NC (CLKN7)	0800 14 Jun	1009.1	0600 14 Jun		53			
Cape San Blas, FL (CSBFI)			0442 12 Jun		35			
Chesapeake Bay, VA (CHLV2)	1000 16 Jun	1007.5	1610 16 Jun	33	34			
Dauphin Island, AL (DPIA1)	1600 11 Jun	1007.5	1420 11 Jun	31	44			
Diamond Shoals, NC (DSLN7)	0900 14 Jun	1013.0	1400 14 Jun		36			
Grand Isle LA (GDIL1)	0900 11 Jun	1005.1	0850 11 Jun	34	45			
Sea Rim State Park, TX (SRST2)			1450 5 Jun	41	53			
Southwest Pass, LA (BURL1)	1100 11 Jun	1004.5	1110 11 Jun	41	49			

TABLE 2. (Continued)

Location	Min sea level pressure		Max surface wind speed			Storm surge (m) ^c	Storm tide (m) ^d	Total rain (mm)
	Time (UTC)/date	Pressure (mb)	Time (UTC)/date	Sustained (kt) ^b	Gust (kt)			
Buoys								
42007 (30.1°N, 88.8°W)			1120 11 Jun	34	49			
42035 (29.3°N, 94.4°W)			1500 5 Jun	31	41			
42040 (29.2°N, 88.2°W)	1100 11 Jun	1008.4	1600 11 Jun	33	41			
44009 (38.5°N, 74.7°W)	1000 17 Jun	1004.4	1330 11 Jun	31	33			
Oil rig platforms								
K7B5 (28.1°N, 93.2°W)			1400 5 Jun	40	50			
K3B6 (28.0°N, 92.8°W)			1445 10 Jun	42				
K7R8 (28.3°N, 92.0°W)			1542 10 Jun		35			

^a Time/date is for sustained wind when both sustained and gust are listed.

^b Except as noted, sustained wind averaging periods for C-MAN and land-based Automated Surface Observing System (ASOS) reports are 2 min; buoy averaging periods are 8 min.

^c Storm surge is water height above normal astronomical tide level.

^d Storm tide is water height above National Geodetic Vertical Datum (1929 mean sea level).

winds near the “eye” and that the radius of maximum winds was approximately 100 n mi—more typical of a subtropical low. Additionally, upper-air data indicated the cyclone remained in a weakly baroclinic environment and lacked full TC structure.

Allison moved east-northeastward across southern Mississippi into southwestern Alabama by 0000 UTC 12 June as it weakened back to a subtropical depression. It continued east-northeastward across southern Alabama, southern Georgia, and southern South Carolina before stalling near Wilmington, North Carolina, on 14 June. The center drifted slowly northward across eastern North Carolina and into southeastern Virginia on 15 June. Allison then accelerated, reaching the Delmarva Peninsula and emerging into the Atlantic on 17 June. At that time, Allison regained subtropical storm status as it began interacting with a frontal system. It merged with the front and became extratropical early on 18 June, then it dissipated southeast of Nova Scotia early the next day.

2) METEOROLOGICAL STATISTICS

Selected surface observations from land stations, Coastal-Marine Automated Network (C-MAN) stations, and data buoys are in Table 2. Allison’s peak intensity on 5 June was based on a 1700 UTC observation of 48 kt from the NOAA ship *McArthur* (call sign WTEJ) and 55-kt measured flight-level and estimated surface winds from a reconnaissance aircraft at 1852 UTC. Surface observations along the northern Gulf coast indicated that Allison had become a subtropical storm on 11 June. In addition, sailboats participating in a race from Annapolis, Maryland, to Newport, Rhode Island, on 17 June reported sustained winds as high as 48 kt and gusts as high as 68 kt at the mouth of Delaware Bay and near Cape May, New Jersey. Although the accuracy of the observations is doubtful due to inconsistency with near-

by official observations, they helped determine that Allison had regained subtropical storm status.

Storm surges of 0.6–0.9 m and accompanying 2.4-m waves caused overwash, beach erosion, and damage to roads on the western portions of Galveston Island not protected by the seawall. Some evacuations were required in this area. A storm surge of 0.3–0.6 m occurred over southeast Louisiana on 11 June.

Twenty-three tornadoes occurred in association with Allison from 11 to 16 June, with 10 tornadoes in South Carolina, 4 in Mississippi, 3 in Florida, 2 in both Alabama and Georgia, and 1 each in Louisiana and Virginia.

The greatest impact from Allison was widespread torrential rainfall and the resulting flooding over much of southeastern Texas, including the Houston metropolitan area, and over portions of southern Louisiana. Several Houston localities reported more than 750 mm of rain (25.4 mm = 1 in.), with the port of Houston receiving 939.5 mm. In Louisiana, Thibodeaux reported a storm total of 758.4 mm. Heavy rain and widespread floods also occurred along the remainder of Allison’s track through the southeastern and eastern United States. This included totals of 257.3 mm at Tallahassee, Florida, and 258.3 mm at Chanfont, Pennsylvania.

3) CASUALTY AND DAMAGE STATISTICS

Allison directly caused 41 deaths, with 23 in Texas, 8 in Florida, 7 in Pennsylvania, and 1 each in Louisiana, Mississippi, and Virginia. Twenty-seven deaths were due to drowning in freshwater floods. One death was due to a tornado in Zachary, Louisiana. There were also nine “indirect” deaths in North Carolina from traffic accidents on wet roads.

The widespread heavy rains produced catastrophic floods over portions of southeastern Texas and significant floods along the remainder of Allison’s track. Dam-

age estimates from the Federal Emergency Management Agency (FEMA) and state emergency management agencies were near \$5 billion, with approximately \$4.9 billion in the Houston metropolitan area. Damage estimates in the Houston area included \$2.04 billion to public facilities (especially the Texas Medical Center), \$1.76 billion to residential properties, and \$1.08 billion to businesses. More than 14 000 homes were destroyed or suffered major damage, and nearly 34 000 homes incurred lesser damage. The damage and direct death toll estimates make Allison the deadliest and most costly tropical or subtropical storm on record in the United States.

4) WARNINGS

Allison formed close to the Gulf coast, which resulted in little warning lead time. A tropical storm warning was issued at 1900 UTC 5 June from Sargent, Texas, eastward along the Gulf of Mexico coast to Morgan City, Louisiana. This was less than 3 h before tropical storm force winds were reported along the upper Texas coast.

Gale warnings were issued for the northeastern Gulf of Mexico about 3 h prior to Allison reaching subtropical storm status on 11 June. The Marine Prediction Center (MPC) in Washington, D.C., also issued gale warnings for portions of the mid-Atlantic offshore waters on 14–15 June when Allison was expected to move off the U.S. east coast and possibly intensify.

Consistent with operational protocol, the NHC transferred responsibility for Allison to the Hydrometeorological Prediction Center (HPC) in Washington, D.C., when the cyclone initially moved inland and weakened. By then, the primary threat was freshwater floods due to the heavy rain. HPC continued to issue products throughout the remainder of Allison's track. Although poststorm analysis shows Allison as a subtropical system over the southeastern United States, the decision for the HPC to retain forecast responsibility was supported by the 1) need for consistency in service source, 2) uncertainty in the assessment of storm type, 3) the short duration of gale force winds on 11 June, and 4) the center remaining over land.

b. Tropical Storm Barry

Barry struck the Florida Panhandle at just under hurricane strength.

1) SYNOPTIC HISTORY

Barry formed from a tropical wave that emerged from the coast of Africa on 24 July. The wave moved westward across the tropical Atlantic with little development until 28 July, when associated convection increased as the wave approached the Lesser Antilles. The system moved into the eastern Caribbean Sea on 29 July ac-

companied by poorly organized thunderstorms and gusty winds. Convection increased further on 30–31 July as the wave moved west-northwestward. It moved into the southeastern Gulf of Mexico on 1 August, accompanied by widespread heavy rains over southern Florida and western Cuba.

A broad 1014-mb low formed along the wave near Dry Tortugas, Florida, late that day, then moved northward and intensified. Postanalysis indicates that the low became a tropical depression early on 2 August approximately 175 n mi west-northwest of Key West, Florida (Fig. 1). Aircraft data indicated the system became Tropical Storm Barry near 1800 UTC that day. A large area of tropical storm force winds existed north and east of the center, due to interaction between the cyclone and a strong surface ridge over the southeastern United States.

Barry may not have been fully tropical during genesis as an upper-level low was over the surface center. Southwesterly upper-level flow moved the upper low northward as Barry moved west-northwestward, steered by flow near the lower-level ridge. The resulting shear and falling environmental surface pressures caused the cyclone to weaken to a depression early on 4 August. Barry remained in a generally unfavorable environment until early on 5 August.

Steering currents collapsed on 3 August, and Barry slowed to a west-southwestward drift over. This was followed by a general northeastward drift the next day. Flow around a mid- to upper-level low dropping southward into the western Gulf states caused Barry to turn northward and accelerate on 5 August.

Convection concentrated near the center early on 5 August, leading to a burst of intensification. The central pressure fell from 1004 to 990 mb in 7 h along with a dramatic improvement in organization in satellite and radar imagery. This short-lived strengthening made Barry a 60-kt cyclone, and this intensity was maintained until landfall near Santa Rosa Beach, Florida, at 0500 UTC 6 August. Radar imagery at that time showed that Barry was forming an eye and had strong convection in the developing northern eyewall.

The cyclone turned northwestward and weakened rapidly after landfall. It became a tropical depression over southern Alabama later on 6 August and a low pressure area near Memphis, Tennessee, the next day. The remnant low dissipated over southeastern Missouri on 8 August.

2) METEOROLOGICAL STATISTICS

The Hurricane Hunters made 35 center "fixes" of Barry. The maximum flight-level winds reported were 71 kt just after landfall. Additionally, an inner-core dropwindsonde measured a surface wind of 61 kt at 1847 UTC on 5 August. The maximum surface winds reported by an official land station were 42 kt with gusts to 69 kt at station C-72 of the Eglin Air Force

TABLE 3a. Tropical Storm Barry, selected surface observations, 2–7 Aug 2001.

Location	Min sea level pressure		Max surface wind speed			Storm surge (m) ^c	Storm tide (m) ^d	Total rain (mm)
	Time (UTC)/date	Pressure (mb)	Time (UTC) ^a /date	Sustained (kt) ^b	Gust (kt)			
Alabama								
Troy (KTOI)								102.9
Florida								
Apalachicola (KAQQ)	0019 6 Aug	1011.9	0739 6 Aug	27	41			162.6
Destin (KDTS) ^f	0449 6 Aug	999.3	0421 6 Aug	31	42			
Crestview (KCEW)	0656 6 Aug	996.6	0603 6 Aug	31	44			55.4
Eglin A-5			0450 6 Aug	28	39			
Eglin C-52	0541 6 Aug	994.2	0525 6 Aug	27	52			
Eglin C-72	0613 6 Aug	995.6	0535 6 Aug	42	69			
Mary Esther (KHRT)	0555 6 Aug	1005.6	0455 6 Aug	24	42			18.0
Panama City (KPFN)	0141 6 Aug	1008.1	0440 6 Aug	26	35			131.8
Tallahassee (KTLH)	0701 6 Aug	1013.5	0222 6 Aug	20	26			226.3
Tyndall AFB (KPAM)	0255 6 Aug	1009.8	2350 5 Aug	25	42			220.4
Valparaiso (KVPS)	0555 6 Aug	998.6	0655 6 Aug	35 ^e	55 ^e			99.6
C-MAN stations/buoys								
Cape San Blas, FL (CSBF1)	0000 6 Aug	1009.8	0340 6 Aug	35 ^g	44			
42003 (25.9°N, 86.9°W)	1000 4 Aug	1009.7	1400 5 Aug	30 ^g	39			
42036 (28.5°N, 84.5°W)	0800 5 Aug	1011.6	2000 2 Aug	29	37			
42039 (28.8°N, 86.1°W)	2000 5 Aug	1001.5	2000 5 Aug	39	54			

^a Time/date is for sustained wind when both sustained and gust are listed.

^b Except as noted, sustained wind averaging periods for C-MAN and land-based ASOS reports are 2 min; buoy averaging periods are 8 min.

^c Storm surge is water height above normal astronomical tide level.

^d Storm tide is water height above National Geodetic Vertical Datum (1929 mean sea level).

^e Estimated.

^f Station disabled by storm—incomplete record.

^g 10-min average.

Base (AFB) mesonet network. Additional selected surface observations from official stations are included in Table 3.

Aircraft data at landfall and an unofficial observation received just after landfall suggested the possibility that Barry had become a hurricane near the time of landfall. The NHC sent a request to the public asking for additional observations from the landfall area. More than 30 supplemental reports were received, with the most significant and useful included in Table 3. Several revealing and much-appreciated wind reports ashore were in the 60–65-kt range, which supported Barry's being on the threshold of hurricane strength, but not actually a hurricane at landfall.

The lowest aircraft-measured pressure was 990 mb, at 1154 UTC 5 August and again at landfall. The lowest pressure from an official station was 994.2 mb from the Eglin AFB mesonet network (Table 3). The unofficial data include a 988.5-mb pressure in Freeport, Florida, and a 989.1-mb observation in Destin. While these reports were lower than any aircraft pressure, the accuracy of these measurements is uncertain. Therefore, the overall minimum pressure is the aircraft-reported 990 mb.

Storm surges and tides from Barry were 0.6–0.9 m near the landfall area in Bay and Walton Counties. Tides of 0.6–0.9 m above normal also occurred along portions

of the southeastern Louisiana coast in association with the strong winds early in Barry's life.

Storm total rainfalls were generally 125–225 mm over the Florida Panhandle near and east of the landfall area with 25–100 mm from southwestern Georgia to northern Mississippi. The maximum amount reported from an official station was 226.3 mm at Tallahassee, Florida. Supplemental observations include 279.4 mm at WJHG-TV in Panama City, Florida, and 243.1 mm at Port St. Joe, Florida. These rains caused localized floods. The pre-Barry tropical wave produced 75–200 mm of rain over portions of southern Florida with local amounts as large as 330 mm in Martin County. These rains helped relieve long-term drought conditions in this area.

One tornado occurred during Barry—an F0 near Carabelle, Florida. The pre-Barry wave produced F0 tornadoes near Fort Pierce and Boynton Beach, Florida. All three tornadoes caused minor damage.

3) CASUALTY AND DAMAGE STATISTICS

Barry directly caused two deaths: one due to a lightning strike in an outer band near Jacksonville, Florida, and one drowning in a rip current at Sanibel Island, Florida. Rains from the storm caused one indirect death in a traffic accident. Additionally, as the pre-Barry wave

TABLE 3b. Tropical Storm Barry, selected unofficial surface observations, 2–7 Aug 2001.

Location	Min sea level pressure		Max surface wind speed			Total rain (mm)
	Time (UTC)/date	Pressure (mb)	Time (UTC)/date	Sustained (kt)	Gust (kt)	
Alabama						
Red Level	0930 6 Aug	1003.0	0818 6 Aug		34	76.2
Florida						
Callaway						197.6
Crestview (Davidson High School)	0824 6 Aug	998.3	0724 6 Aug		35	
DeFuniak Springs	0630 6 Aug	997.9				116.8
Destin		989.1		62 ^c	69	
Destin 5–10 s mi E			0440 6 Aug	48	63	
Destin AWS	0435 6 Aug	1004.1	0500 6 Aug		40	
Destin Harbor ^a			0500 6 Aug	65	75	
Fort Walton Beach (Choctawhatchee High School)		1002.7	0613 6 Aug		35	
Freeport	0440 6 Aug	988.5				
Hiland Park		1007.8				138.4
Lynn Haven						198.1
Mary Esther 3 SSW s mi KHRT						132.1
Miramar Beach	0503 6 Aug	991.8		57	73	
Niceville			0440 6 Aug		57	
Panama City Bay High School						165.9
Panama City, the Cove						242.8
Panama City, WJHG-TV						279.4
Phillips Inlet				64 ^d		102.9
Port St. Joe						243.1
Santa Rosa Beach			0426 6 Aug		70	
Seagrove Beach			0450 6 Aug	82 ^c	93	
St. Andrews State Park ^b		991.8	0310 6 Aug	63 ^c		
St. George Island						113.8
Wasuau 3 s mi E						223.5

^a Time/date is for sustained wind when both sustained and gust are listed.

^b Sailboat, likely with nonstandard anemometer elevation.

^c 3-min average.

^d 1-min average.

^e 4-min average.

moved over Cuba and the Straits of Florida, the accompanying winds and seas capsized a boat with Cuban refugees on board. Press reports indicated that 6 of the 28 passengers drowned.

The American Insurance Services Group estimated insured property damage from Barry to be \$15 million. Applying the NHC historical estimate of a 2:1 ratio of total damage to insured damage, the total damage from Barry was estimated to be \$30 million.

4) WARNINGS

Hurricane warnings were issued for portions of the northern Gulf coast in anticipation that Barry's strengthening on 5 August would continue. These were somewhat short-fused with a lead time of about 16 h before landfall. Tropical storm watches and warnings were issued along portions of the Louisiana and Mississippi coasts in response to early forecasts suggesting Barry would threaten those areas.

c. Tropical Storm Chantal

Chantal showed considerable variations in strength during its life. It made landfall in Belize at just below hurricane strength.

1) SYNOPTIC HISTORY

Chantal developed from a tropical wave that moved westward off the coast of Africa on 11 August. A broad surface low and closed circulation developed by 13 August, with convection increasing northwest of the center early on 14 August. The system became a tropical depression at 1800 UTC that day about 1300 n mi east of the southern Windward Islands (Fig. 1). South of a strong midlevel ridge, the depression moved westward at about 23 kt. Vertical wind shear slowed development for the next 36 h. This was followed by increased organization early on 16 August. However, reconnaissance aircraft data could not find a closed circulation in the system around 2100 UTC that day, which by then was moving near 30 kt. It cannot be determined precisely

when the depression degenerated into an open wave, but QuikSCAT data suggest it may have been near 1200 UTC 16 August, even though some Dvorak intensity estimates indicated tropical storm strength at that time.

The wave sped through the Windward Islands early on 17 August, then decelerated to 20 kt over the south-eastern Caribbean Sea as the convective pattern expanded and became more symmetric. At 1400 UTC, a reconnaissance aircraft found that a small closed circulation with 35-kt winds about 250 n mi south of St. Croix. The wave had become a tropical storm.

Over the next 18 h the pressure fell from 1010 to 1003 mb and maximum winds increased to 55 kt. During the morning of 18 August, however, Chantal weakened slightly as its forward speed increased to 24 kt and the low-level center raced ahead of the deep convection. This was followed by a second episode of slowing and strengthening ending at 0600 UTC 19 August, when the pressure was 997 mb and the maximum winds 60 kt. At this time, Chantal was moving westward at 12 kt about 160 n mi south of Kingston, Jamaica. It is possible that the apparent reduction in forward speed resulted from reorganization or reformation of the low-level circulation.

Later that day, Chantal again became disorganized with an ill-defined center located well west-southwest of the main area of deep convection. Although the pressure rose to 1008 mb, reconnaissance aircraft encountered strong winds in the convection. Chantal turned west-northwestward across the northwestern Caribbean. It maintained a near steady-state structure with 50-kt winds until late on 20 August. During this period, there were differences (often 60 n mi or more) between aircraft- and satellite-based position fixes.

Chantal became much better organized as it approached Belize and the Yucatan Peninsula late on 20 August. The center became well defined and the strongest winds edged closer to the center than previously. This occurred as yet another deceleration occurred, and was accompanied by diminishing vertical shear. The center came ashore near the Belize–Mexico border around 0200 UTC 21 August with maximum winds estimated at 60 kt. After landfall, the forward speed slowed further, and radar data from Belize showed continued increasing organization for several hours. Chantal would likely have become a hurricane had it remained over water for another hour or two.

Over the next 36 h, the cyclone moved westward and then southwestward over the Yucatan and southeastern Mexico, weakening to a depression at 0000 UTC 22 August and dissipating 18 h later.

2) METEOROLOGICAL STATISTICS

Chantal twice reached a maximum intensity of 60 kt. In the first instance, the peak flight-level wind from reconnaissance aircraft in Chantal was 82 kt, measured at a flight level of 850 mb at 1123 UTC 19 August.

Although the standard reduction for this altitude would indicate surface winds of hurricane force (Franklin et al. 2000), several factors suggest a lower intensity. First, the area of flight-level winds that supported hurricane intensity was extremely limited and may not have been representative of the cyclone's overall circulation. Second, Chantal's minimum pressure was rising rapidly at the time; this is consistent with the aircraft-observed wind being primarily a local convective, rather than a cyclone-scale, event. The most convincing evidence, however, comes from soundings in the storm core and environment in the right semicircle, which showed significant low-level shear. The Kingston sounding from 1200 UTC 18 August showed about 20 kt of easterly shear between 925 and 700 mb. A dropwindsonde at 2340 UTC 19 August reported 700-mb winds of 60 kt and a surface wind of only 38 kt. In this environment, a larger than normal surface wind reduction would be appropriate on the right-hand side of the cyclone.

Chantal also reached an intensity of 60 kt just prior to landfall. This estimate is supported by a dropwindsonde surface wind of 58 kt, and a surface-adjusted flight-level wind of 57 kt. Dropwindsonde profiles at this time indicate that the surface adjustment factors had returned to more typical values. The estimated landfall pressure of 999 mb is based on extrapolation of the deepening trend observed by aircraft up until the last report of 1001 mb at 2307 UTC 20 August.

The strongest winds at landfall in the western Caribbean were likely in a band roughly 30–40 n mi north of the center, near Chinchorro Banco, Mexico. Unfortunately, there are no observing stations in this area. Caye Caulker, Belize, reported a gust of 62 kt, and Chetumal, Mexico, reported a gust of 54 kt. In the Lesser Antilles, the automated station on Martinique (78922, station elevation 33 m) reported a 10-min sustained wind of 34 kt at 0600 UTC 17 August.

Chantal produced copious rain, with a storm total of 340.6 mm reported from Chetumal. Several sites in Belize reported totals in the 200–250-mm range.

3) CASUALTY AND DAMAGE STATISTICS

Chantal caused no official deaths as a TC. However, lightning killed two people in Trinidad as the tropical wave passed through the Lesser Antilles.

Damage in Belize was estimated near \$4 million, primarily from wave damage to seawalls and piers, agricultural losses from wind and floods, and erosion of roads due to floods. About 8000 people were evacuated, mainly from offshore islands. About 2500 persons were evacuated from vulnerable areas in Mexico. Reports from Mexico indicated downed trees but no significant damage otherwise.

4) WARNINGS

Tropical storm warnings were issued for portions of the Lesser Antilles. These warnings were discontinued

when the cyclone weakened to a tropical wave. A hurricane warning was issued for Jamaica and a tropical storm warning for the Cayman Islands based on forecasts that incorrectly anticipated a close approach to those islands. Tropical storm warnings were issued for Belize and the Yucatan Peninsula about 23 h before Chantal made landfall near the Mexico–Belize border, roughly in the center of the warning area. A tropical storm warning was issued for a portion of the Gulf coast of Mexico in anticipation of Chantal's reemergence over water into the Gulf of Mexico. However, Chantal remained over land.

d. Tropical Storm Dean

Dean developed from a fast-moving, strong tropical wave that moved westward from the coast of Africa on 14–15 August. On 21 August, the wave moved through the northern Leeward Islands with tropical storm force wind gusts, but surface, radar, and aircraft data indicated the system did not have a closed low-level circulation. On 22 August, surface and aircraft data indicated a closed circulation near the U.S. Virgin Islands around 1200 UTC, and the system became Tropical Storm Dean (Fig. 1). Maximum sustained winds reached 50 kt later that day. Dean then weakened as quickly as it had developed. A reconnaissance aircraft was unable to find a closed circulation on 23 August. The remnant area of disturbed weather moved northward for the next 3 days beneath hostile upper-level shear. By 26 August, the system had become a nearly stationary broad low and thunderstorm activity began to redevelop near the center. The low became a tropical depression and then regained tropical storm status early on 27 August. Dean reached its maximum intensity of 60 kt later that day about 350 n mi north-northeast of Bermuda. Afterward, the northeastward-moving Dean gradually weakened over colder water. It became extratropical on 28 August and merged with a larger extratropical low well east of Newfoundland the next day.

St. Thomas in the U.S. Virgin Islands reported 35-kt sustained winds with gusts to 42 kt, and a gust to 63 kt was reported on top of a 90-m-high hill on St. Croix. The ship *Lykes Navigator* reported 55-kt winds and a 1004.0-mb pressure at 0600 UTC 27 August. This observation helped confirm that Dean had regained tropical storm strength.

A tropical storm warning was issued for the southeastern Bahamas as Dean approached on 22 August. This was canceled when the system weakened. There were no reports of casualties from Dean, but heavy rain produced widespread floods across much of Puerto Rico. Several major highways were inundated and 1320 homes were flooded. Agricultural losses totaled about \$2 million. In the U.S. Virgin Islands, there were numerous power outages, small trees blown down, and some roads damaged.

e. Hurricane Erin

Erin can be traced back to a vigorous tropical wave that left the African coast on 30 August. Over the next 2 days, a low pressure system accompanying the wave became better defined as thunderstorm activity organized near the low-level center. The system became a tropical depression at 1800 UTC 1 September about 600 n mi west-southwest of the Cape Verde Islands (Fig. 1) and became Tropical Storm Erin about 12 h later. Erin reached an initial peak intensity of 50 kt on 3 September, then slowly weakened as the cyclone moved west-northwestward in a moderate westerly shear environment. The shear caused Erin to degenerate into an area of disturbed weather on 5 September about 240 n mi east-northeast of the northern Leeward Islands. The disturbance turned northward and a new center developed on 6 September about 400 n mi north-northeast of the northern Leeward Islands. Erin regained tropical depression status near 1800 UTC that day and tropical storm status 24 h later. Moving north-northwestward, Erin became a hurricane late on 8 September. Maximum winds reached 105 kt the next day as it passed about 80 n mi east-northeast of Bermuda (Fig. 3). Erin continued north-northwestward and slowly weakened, then recurved sharply east-northeastward on 11 September. The hurricane maintained this motion until 13 September when a strong upper-level trough caused it to accelerate northeastward and weaken (Fig. 4). Erin passed just east of Cape Race, Newfoundland, as a 60-kt tropical storm around 0000 UTC 15 September. The cyclone became extratropical shortly thereafter, eventually merging with a larger extratropical cyclone on 17 September near the southern coast of Greenland.

Erin's close approach to Bermuda required a hurricane warning for the island. Although the island was only 80 n mi from the center, it was on the weaker side of the storm and the maximum reported wind was a gust to 36 kt. Cape Race reported 46-kt sustained winds with a gust to 58 kt on 15 September just after Erin became extratropical. The ship *Semyonovsk* (call sign UCTR) reported 48-kt winds at 1500 UTC 14 September. Rainfall totals were 75–125 mm in southeastern Newfoundland. There were no reports of damages or casualties.

f. Hurricane Felix

A tropical wave and accompanying weak surface low moved westward from the coast of Africa on 5 September. The system gradually became better organized, and it became a tropical depression on 7 September about 360 n mi southwest of the Cape Verde Islands (Fig. 1). As the system moved west-northwestward, it encountered strong upper-level southwesterly winds, which caused it to degenerate back into a tropical wave on 8 September. The wave moved westward and redeveloped into a tropical depression on 10 September about 870 n mi east of the Lesser Antilles. The cyclone became

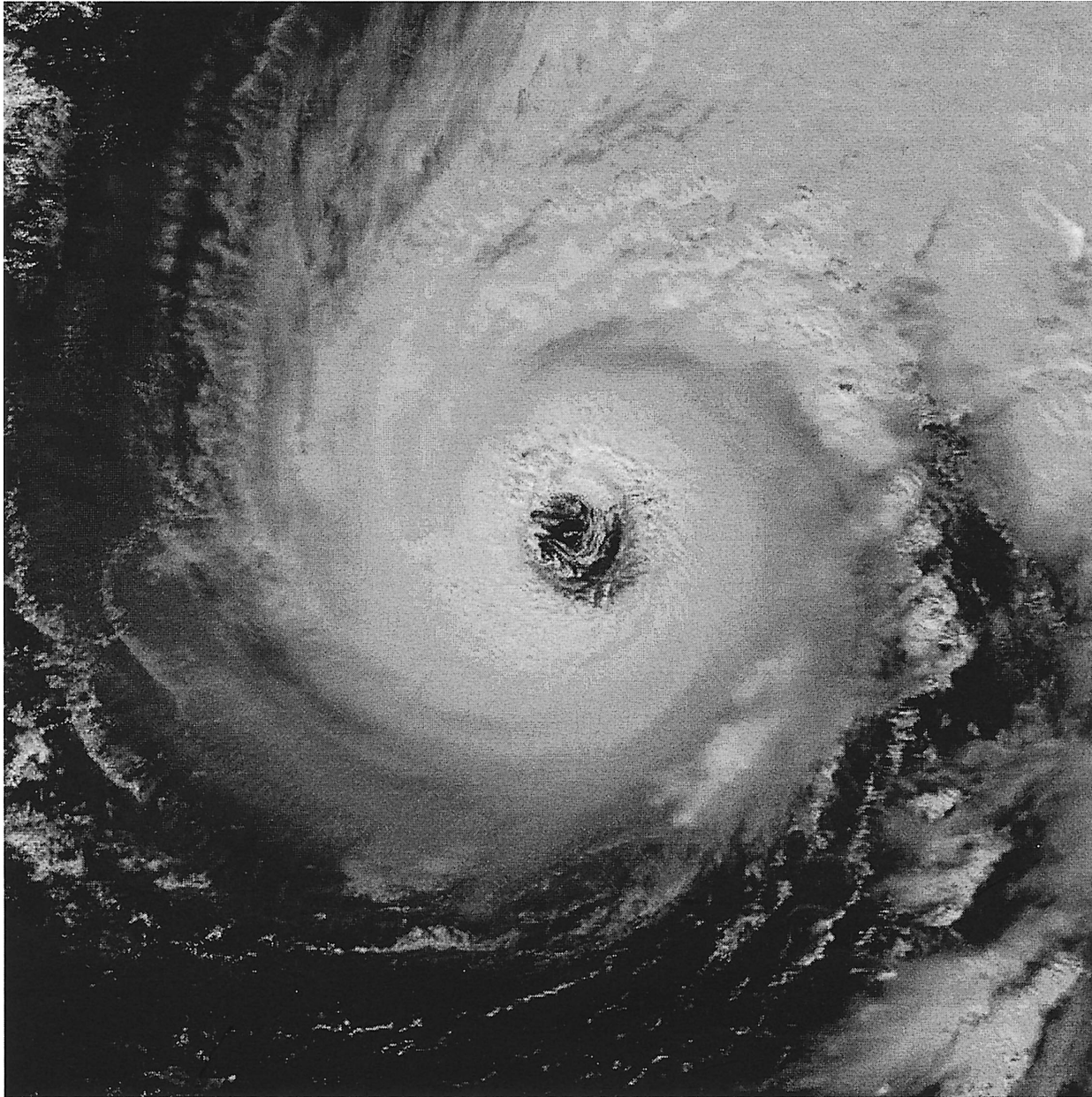


FIG. 3. Moderate Resolution Imaging Spectroradiometer (MODIS) 1-km $0.66\text{-}\mu\text{m}$ image of Hurricane Erin, from the *Terra* (Earth Observing System AM-1) polar-orbiting satellite at 1530 UTC 9 Sep 2001. MODIS data acquired by direct broadcast from the NASA *Terra* spacecraft at the Space Science and Engineering Center, University of Wisconsin—Madison.

Tropical Storm Felix the next day as it turned northward, followed by a northward turn on 12 September. It became a hurricane on 13 September about 1300 n mi southwest of the Azores Islands (Fig. 4), and its maximum winds reached 100 kt the next day. Soon thereafter, Felix turned east-northeastward and slowly weakened, with the cyclone becoming a tropical storm on 17 September. Felix became nearly stationary about 300 n mi southwest of the Azores on 18 September. Increasing vertical wind shear and cold water upwelling brought about rapid weakening, and Felix weakened to

a depression later that day. It degenerated into a non-convective low pressure system early on 19 September about 350 n mi southwest of the Azores.

g. Hurricane Gabrielle

Gabrielle hit the west coast of the Florida peninsula at just under hurricane strength. It later became a hurricane in the Atlantic.

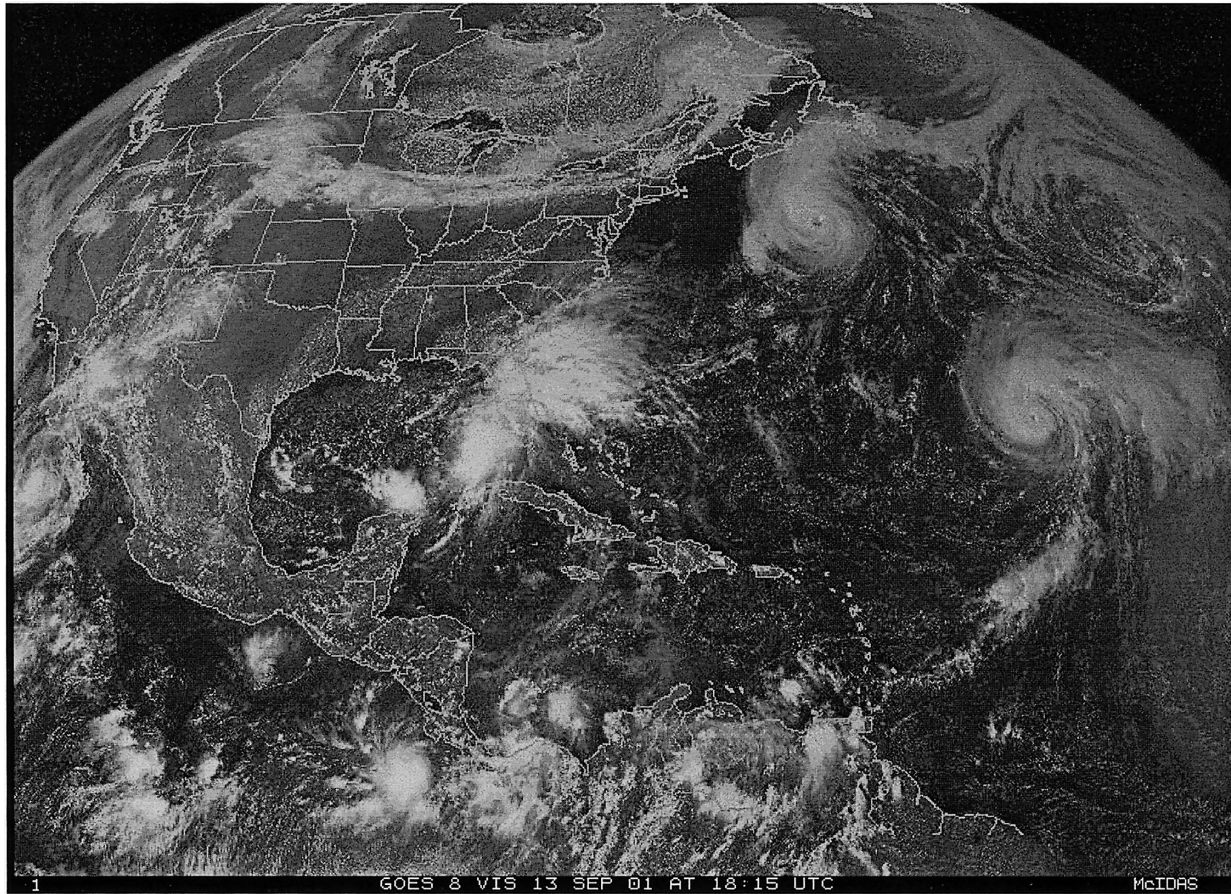


FIG. 4. GOES-8 visible image of Hurricane Erin (in the northern Atlantic southeast of Nova Scotia), Hurricane Felix (in the central Atlantic), and Tropical Storm Gabrielle (in the Gulf of Mexico) at 1815 UTC 13 Sep 2001, provided by the National Climatic Data Center.

1) SYNOPTIC HISTORY

Gabrielle's origin was nontropical. On 5 September, a weak low- to midlevel trough was nearly stationary just east of the southeastern U.S. coast. This feature persisted and developed into a low- to midlevel cutoff low over Florida by 9 September. Late on 11 September, the cutoff low spawned a surface low over the southeastern Gulf of Mexico with sufficiently well-organized convection to classify the system as a tropical depression (Fig. 1).

Within a weak steering flow, the cyclone made a small counterclockwise loop over the southeastern Gulf for about 60 h and gradually strengthened. It reached tropical storm strength on 13 September about 175 n mi southwest of Venice, Florida (Fig. 4). By this time, a midlevel westerly trough was moving into the eastern United States and helped Gabrielle accelerate northeastward. Landfall occurred near Venice at about 1200 UTC 14 September. Strengthening had continued despite westerly vertical shear, and maximum sustained winds reached 60 kt just before landfall.

Gabrielle decelerated and its winds decreased to 40 kt during its 18-h traverse of the central Florida pen-

insula. The center moved off the Florida east coast near Titusville and accelerated northeastward. Although the cyclone was sheared and had an atypical structure for a TC, Gabrielle gradually strengthened into a hurricane with 70-kt winds on 17 September about 200 n mi northwest of Bermuda.

Continuing northeastward, Gabrielle weakened to a tropical storm on 18 September and became extratropical early the next day about 300 n mi south of Newfoundland. The cyclone later passed near southeastern Newfoundland before merging with another extratropical low on 21 September over the far north Atlantic Ocean.

2) METEOROLOGICAL STATISTICS

Gabrielle brought tropical storm force winds to portions of the Florida peninsula. An automated station at Port Manatee, Florida, reported 52-kt sustained winds with a gust to 63 kt, and the C-MAN station at St. Augustine, Florida, reported 51 kt sustained winds with a gust to 65 kt. A University of South Florida buoy located southwest of Venice reported 44-kt sustained

TABLE 4. Selected surface observations for Hurricane Gabriele, Sep 2001.

Location	Min sea level pressure		Max surface wind speed			Storm surge (m) ^c	Storm tide (m) ^d	Total rain (mm)
	Time (UTC)/date	Pressure (mb)	Time (UTC)/date	Sustained (kt) ^b	Gust (kt)			
Florida								
Amelia Island				52				
Apopka								140.5
Avalon								113.0
Brooksville (KBKV)	1845 15 Sep	998.6	0135 15 Sep	25	40			
Bunnell			0619 15 Sep	31	42			
Canaveral Trident	0900 15 Sep	998.2	2100 14 Sep		37			
Cecil Field (KNZC)	0039 15 Sep	1004.1	0906 15 Sep	30	39			
Charlotte County						1.6	1.9	
Clearwater Beach			1436 14 Sep	38	47			
Crescent City								131.6
Daytona Beach (KDAB)	1647 14 Sep	998.6	1052 14 Sep	37	43			195.3
Egmont Key (USF)			1615 14 Sep	46				
Everglades City	1200 14 Sep	1000.0	1200 14 Sep	44	61			
Fernandina Beach	0500 15 Sep	1005.2	1000 15 Sep	28	36			
Flagler Beach Fire Station	0900 15 Sep	999.7						
Flamingo	1000 14 Sep	1002.4	0900 14 Sep	45	54			
Fort Myers (KFMY)	1046 14 Sep	996.3	1208 14 Sep	31	40			
Fort Myers (KRSW)	1144 14 Sep	998.6	1007 14 Sep	27	38			
Fort Pierce (KFPR)	0504 15 Sep	999.6	0244 15 Sep	24	33			50.0
Gainesville (KGNV)	2331 14 Sep	1002.4	2044 14 Sep	24	29			
Hastings			2100 14 Sep	20				
Jacksonville (KJAX)	0459 15 Sep	1004.7	0412 15 Sep	29	36			
Jacksonville, Craig Airport (KCRG)	0707 15 Sep	1003.7	0848 15 Sep	27	36			
Jacksonville NAS (KNIP)	0701 15 Sep	1003.0	0927 15 Sep	34	41			
Key West						0.2		
Key West International Airport (KEYW)	0929 14 Sep	1003.7	0929 14 Sep	36	42			24.1
Lakeland (KLAL)	1650 14 Sep	994.2	1450 14 Sep	20	45			
Lee County						1.0	1.2	
Leesburg	1538 14 Sep	995.6	0045 15 Sep	31	39			202.7
Marathon (KMTH)	1009 14 Sep	1005.4	1052 14 Sep	23	39			31.2
Macdill AFB (KMCF)	1458 14 Sep	996.3	1148 14 Sep	21	40			
Mayport Coops	0600 15 Sep	1003.7	2300 14 Sep	36	46			
Mayport NAS (KNRB)	0507 15 Sep	1003.4	0402 15 Sep	41	47			
Melbourne (KMLB)	0519 15 Sep	997.9	1623 14 Sep	25	35			106.2
Naples (KAPF)	0950 14 Sep	999.4	1146 14 Sep	24	41			77.7
Naples Coops	1000 14 Sep	998.9	0900 14 Sep	32	47			
New Pass	1245 14 Sep	996.1	1207 14 Sep	51				
NW FL Bay COMPS	0900 14 Sep	1003.1	1400 14 Sep	33	42			24.1
Ochopee								109.2
Okahumpka								231.1
Orlando Executive Airport (KORL)	1516 14 Sep	995.2	1326 14 Sep	27	36			120.4
Orlando International Airport (KMCO)	1412 14 Sep	994.5	1254 14 Sep	31	39			102.1
Palatka								156.7
Palm Coast								194.3
Palmetto								295.9
Patrick AFB (KCOF)	0755 15 Sep	998.0	1421 14 Sep	39	86			159.0
Pierson								346.7
Pinellas County						0.3	0.9	
Port Manatee PORTS			1506 14 Sep	52	63			
Punta Gorda (KPGD)	1227 14 Sep	993.9	1212 14 Sep	42	49			
Sanford (KSFB)	1522 14 Sep	995.9	1525 14 Sep	27	33			128.0
Sarasota (KSQR)	1310 14 Sep	991.2	1528 14 Sep	41	54			210.6
Shuttle Landing Facility (KTTS)	0755 15 Sep	998.0	1841 15 Sep	22	36			115.8
St. Augustine (KSGJ)	0800 15 Sep	1003.2	2300 14 Sep	46	64			
St. Petersburg (KPIE)	1321 14 Sep	998.3	1609 14 Sep	36	47			
St. Petersburg (KSPG)	1446 14 Sep	995.9	1521 14 Sep	38	50			

TABLE 4. (Continued)

Location	Min sea level pressure		Max surface wind speed			Storm surge (m) ^c	Storm tide (m) ^d	Total rain (mm)
	Time (UTC)/date	Pressure (mb)	Time (UTC) ^a /date	Sustained (kt) ^b	Gust (kt)			
Tampa (KTPA) Tavares	1525 14 Sep	997.0	1603 14 Sep	32	43			209.8
Titusville (KTIX) Umatilla	1950 14 Sep	998.3						322.8
Vero Beach (KVRB)	0454 15 Sep	998.9	1346 14 Sep	29	37			54.6
Villages, The	2025 14 Sep	996.0	2325 14 Sep	26				
Winter Haven (KGIF)	1752 14 Sep	992.6	1223 14 Sep	35	42			
Georgia								
Kings Bay Naval Station (KNBQ)	0627 15 Sep	1005.1	0413 15 Sep	23	35			
St. Simons Island	0449 15 Sep	1005.8	0532 15 Sep	34	42			
C-MAN stations								
Cedar Key, FL (CDRF1)	2000 14 Sep	1002.9	1920 13 Sep	25 ^e	31			
Dry Tortugas, FL (DRYF1)	0800 14 Sep	1001.7	0300 14 Sep	38	47		64.5	
Long Key, FL (LONF1)	1100 14 Sep	1005.1	1230 14 Sep	30 ^e	45	0.3		
Molasses Reef, FL (MLRF1)	1000 14 Sep	1004.7	1310 14 Sep	36 ^e	45			
Sand Key, FL (SANF1)	0800 14 Sep	1003.1	1020 14 Sep	36 ^e	44			
Sombrero Key, FL (SMKF1)	1000 14 Sep	1004.7	1050 14 Sep	44 ^e	57	0.3		
St. Augustine, FL (SAUF 1)	2200 14 Sep	999.1	2220 14 Sep	51 ^e	65			
Venice, FL (VENF1)	1200 14 Sep	983.1	1400 14 Sep	50	63			
Buoys								
41009 (28.5°N, 80.2°W)	0900 15 Sep	997.7	1500 14 Sep	33	44			
41010 (28.9°N, 78.5°W)	2000 15 Sep	1000.7	1600 15 Sep	27	35			
42003 (25.9°N, 86.9°W)	2100 13 Sep	1003.3	0200 14 Sep	27	35			
42036 (28.5°N, 84.5°W)	1200 14 Sep	1005.2	1200 14 Sep	29	37			
CM3 (USF, 26.1°N, 83.1°W)	0744 14 Sep	992.1	0429 14 Sep	36				
NA2 (USF, 27.2°N, 82.9°W)			1210 14 Sep	44	85			

^a Time/date is for sustained wind when both sustained and gust are listed.

^b Except as noted, sustained wind averaging periods for C-MAN and land-based ASOS reports are 2 min; NOAA buoy averaging periods are 8 min. University of South Florida (USF) buoy averaging periods vary from 1 to 15 min.

^c Storm surge is water height above normal astronomical tide level.

^d Storm tide is water height above National Geodetic Vertical Datum (1929 mean sea level).

^e 10-min average.

winds with a gust to 85 kt at 1210 UTC 14 September. Selected surface observations from Florida are listed in Table 4. Gabrielle also affected shipping, with the ship KRPPD (name unknown) reporting 58-kt winds at 0000 and 1800 UTC 16 September.

While aircraft data are normally the most reliable data in a TC, these observations are occasionally problematic. On 14 September, as Gabrielle approached the west coast of Florida, aircraft 700-mb flight-level winds suggested that surface winds might be near 65 kt. However, coincident surface observations showed significantly lower winds. The estimated wind speed of 60 kt at 1200 UTC at landfall is a compromise between the aircraft and surface observations. This intensity estimate is uncertain and it is possible that Gabrielle was briefly a hurricane near landfall.

The maximum intensity of 70 kt over the Atlantic is based on aircraft dropsonde and flight-level winds. The maximum flight-level wind speed was 85 kt at 850 mb around 1700 UTC 17 September. The standard reduction to the surface under deep convection is 80%, which yields a 68-kt surface wind (Franklin et al. 2000). A

few hours earlier, a dropsonde indicated a surface wind speed of 60 kt.

The lowest central pressure measured by an aircraft was 980 mb at 1009 UTC 14 September. The aircraft weather officer also reported a 972-mb central pressure extrapolated from flight level at 0850 UTC, accompanied by a temperature spike. This value, likely associated with a mesoscale convective event, is not considered to be representative of the actual central pressure.

Storm surges of 1–2 m flooded portions of the western coast of the Florida peninsula, including Charlotte Harbor and the Peace River in Charlotte County and the coast of Lee County. These surges affected several hundred homes and other coastal property.

Florida rainfall totals were generally 100–175 mm over a swath along the storm track. More than 300 mm fell on Volusia and Lake Counties in northeast Florida with a total of 345.4 mm from Pierson. These rains were caused by a combination of Gabrielle and strong northeasterly flow prior to the storm. This flow, combined with the storm winds, high astronomical tides, and rainfall, caused near record floods on the lower St. Johns

River. The rain over west-central Florida resulted in major floods on the Manatee River, Little Manatee River, Myakka River, Peace River, and Horse Creek. A river gauge at Arcadia on Horse Creek reported a crest of 5.1 m, which is 1.5 m above flood stage. Minor river and urban flooding occurred elsewhere along the path of the storm across Florida.

After becoming extratropical, the storm brought more than 150 mm of rain in 12 h or less to the Avalon Peninsula of Newfoundland. Cape Race reported 48.3 mm in 1 h.

Eighteen tornadoes occurred across central and northeastern Florida due to Gabrielle: 16 F0s and 2 F1s. The cyclone also produced five waterspouts: three in the Florida Keys and two along the northeastern Florida coast.

3) CASUALTY AND DAMAGE STATISTICS

Two deaths are directly attributed to Gabrielle. Heavy rains caused a death in a flooded stream in Seminole County, Florida, on 15 September, while swells contributed to a death in a rip current at the Alabama coastline on 13 September. One indirect death was associated with Gabrielle in the Florida Keys when a person fell overboard from a boat and drowned. This death was considered indirect, as local officials determined that intoxication was a greater factor than high winds or seas.

The insured loss total of \$115 million in Florida from wind, rain, and storm surge was reported by the Property Claim Services of the American Insurance Services Group. The total damage estimate was \$230 million.

4) WARNINGS

Tropical storm warnings were issued for the Florida west coast at 2100 UTC 13 September and landfall occurred 15 h later at 1200 UTC 14 September.

h. Hurricane Humberto

Humberto formed along a trough of low pressure that extended southwestward from Hurricane Gabrielle. The trough was about 600 n mi south-southeast of Bermuda on 18 September when a westward-moving upper-level low increased the associated deep convection. A surface low formed in this area the next day and drifted westward. The system gradually became better organized and developed into a tropical depression around 1200 UTC 21 September about 425 n mi south of Bermuda (Fig. 1). The cyclone turned northwestward that day, with aircraft data indicating a weak and disorganized system despite an impressive appearance in satellite imagery. Surface development appeared to catch up to the satellite signature on 22 September and the depression became Tropical Storm Humberto. Moving around the periphery of the subtropical ridge, Humberto turned north-northwestward and gradually strengthened, be-

coming a hurricane on 23 September. It then turned north-northeastward and reached its first peak in intensity, 85 kt and 983 mb, early on 24 September.

Increasing westerly shear caused the cyclone to weaken later that day as it turned northeastward. Humberto entered a less hostile environment on 25 September. Northward motion into a region of light shear associated with an upper-level ridge on 26 September allowed the hurricane to reintensify and reach its maximum intensity of 90 kt. This occurred about 175 n mi south-southeast of Sable Island, Nova Scotia, over water temperatures no higher than 25°–26°C. Deep-layer westerly flow impinging on the storm later that day turned Humberto quickly eastward and increased the vertical shear. Humberto weakened to a tropical storm on 27 September and degenerated into an open trough late that day.

Humberto was heavily sampled by aircraft participating in the joint NOAA/NASA Hurricanes at Landfall/CAMEX4 experiment conducted under the U.S. Weather Research Program. The first peak intensity on 24 September is based on a dropwindsonde surface report of 87 kt, which was consistent with data from the Stepped Frequency Microwave Radiometer on board the NOAA WP-3D aircraft. Humberto passed 120 n mi west of Bermuda, which reported a wind gust to 37 kt on 24 September.

i. Hurricane Iris

Hurricane Iris was a small category-4 hurricane in the western Caribbean that devastated parts of southern Belize.

1) SYNOPTIC HISTORY

Iris formed from a poorly defined tropical wave that moved westward across the tropical Atlantic near the end of September. A large upper-level trough prevailed over the Atlantic with an embedded low just northeast of the Lesser Antilles, creating a hostile upper-level wind environment. When the wave reached 50°W on 3 October, the upper low detached from the trough and moved southwestward over the eastern Caribbean Sea. This resulted in the development of an upper-level ridge over the wave, which provided a more favorable environment. As this occurred, thunderstorm activity increased and a midlevel circulation developed. This circulation gradually developed downward and it is estimated that a tropical depression with a poorly defined center formed about 85 n mi southeast of Barbados at 1200 UTC 4 October (Fig. 1).

The depression and accompanying squalls moved west-northwestward through the southern Windward Islands. It is estimated that the cyclone became a tropical storm at 1200 UTC 5 October about 240 n mi south-southeast of San Juan, Puerto Rico. Iris then became a hurricane near the Barahona Peninsula of the Dominican Republic at 1800 UTC 6 October.

A well-established midlevel ridge north of Iris strengthened and forced the cyclone to move westward. The small core of Iris passed just south of Jamaica during the morning of 7 October. Iris's subsequent track through the northwestern Caribbean Sea placed it in a low-shear environment and over a region of very high upper-oceanic heat content (Mainelli et al. 2002). Rapid intensification began, with the minimum central pressure dropping from 990 to 950 mb and the winds increasing from 75 to 120 kt in about 18 h. This made the west-southwestward moving Iris a category-4 hurricane on the SSHS by 1200 UTC 8 October.

Near the time of this peak in intensity, an aircraft reported three small concentric eyewalls. About an hour later the inner eyewall collapsed with maximum winds temporarily decreasing to 115 kt. Iris then strengthened to its maximum intensity of 125 kt just before landfall near Monkey River Town, Belize (about 60 n mi south of Belize City), around 0200 UTC 9 October (Fig. 5). The cyclone continued westward after landfall and weakened rapidly over the mountains of Central America. The low-level center dissipated by 1800 UTC 9 October. However the remnants of Iris spawned Tropical Storm Manuel over the eastern Pacific a day later (Avila et al. 2003).

2) METEOROLOGICAL STATISTICS

The core of Iris was always small. The initial reconnaissance flight had difficulty finding a closed circulation despite a well-defined appearance in satellite imagery. Iris was upgraded to a hurricane at 1800 UTC 6 October based on an aircraft report of 82-kt winds at 460-m flight level and the presence of a closed eyewall near that time. Iris was upgraded to a category-4 hurricane based on a 134-kt 700-mb flight-level wind. The eye of Iris was as small as 4 n mi across, so some dropsondes released in the eye did not remain there as they fell. The 948-mb minimum pressure is based on extrapolation from the surface pressures and winds of these just-outside-the-eye dropsondes. Iris's peak intensity of 125 kt is based on a 127-kt dropwindsonde surface wind and objective satellite intensity estimates between 127 and 140 kt that lasted about 3 h.

Few surface observations were available from the landfall area or from ships at sea. The maximum wind reported was a gust of 92 kt from an unofficial observer in Big Creek, Belize (16.5°N, 88.4°W), at 0200 UTC 9 October.

3) CASUALTY AND DAMAGE STATISTICS

Damage was concentrated within a 60 n mi wide area mainly in the southern portion of Belize. The *Belize Times* reported that Monkey River Town, Placencia, and Independence were the hardest hit, experiencing a 2.5–4.5-m surge and severe destruction. Many homes in

Monkey River Town and Placencia were destroyed, as was the banana crop in the landfall area.

Iris directly caused 31 deaths. The 37-m boat *M/V Wave Dancer*, with 28 people on board, capsized in port near Big Creek. Twenty of those aboard died. Three people were killed in the Dominican Republic by the cyclone and press reports indicate at least eight people were killed by flash flooding in Guatemala. A total of \$66.2 million in damage was reported by the government of Belize. There were no reports of damage elsewhere.

4) WARNINGS

Tropical storm watches and warnings were issued for the Dominican Republic and Haiti at 1500 UTC 5 October. A hurricane warning was issued for portions of Haiti 6 h later. A hurricane warning was issued for Jamaica at 1500 UTC 6 October, 21 h before the closest approach of the center. Hurricane watches were issued for the Yucatan Peninsula and portions of Belize at 1500 and 1800 UTC 7 October, respectively. These were extended to cover all of Belize at 0000 UTC 8 October. A hurricane warning was issued for Belize at 0300 UTC 8 October or about 23 h before the center made landfall. A hurricane warning was issued for the northern coast of Honduras and Guatemala at 0900 UTC that day due to Iris turning west-southwestward. A tropical storm warning was issued for portions of the Yucatan Peninsula at 1500 UTC 8 October. Hurricane warnings were also issued for portions of southeastern Cuba and the Cayman Islands in anticipation that Iris would move farther north than it actually did.

j. Tropical Storm Jerry

A tropical wave moved westward from the coast of Africa on 1 October. Little change in organization occurred until the wave was near 40°W on 4 October, when the associated deep convection increased and exhibited some curvature. Further development was slow until 6 October, when the system became a tropical depression about 540 n mi east-southeast of Barbados (Fig. 1). The system moved west-northwestward and became Tropical Storm Jerry early on the next day. Jerry passed through the Windward Islands early on 8 October at its maximum intensity of 45 kt. After that, northwesterly vertical shear disrupted the outflow and the convection. Jerry weakened quickly and degenerated into a tropical wave later that day.

Tropical storm warnings were required for the Windward Islands and Tobago. However, the impact was minimal with no reports of damage or casualties. The highest wind speed reported by aircraft at 300-m altitude was 56 kt at 2013 UTC 7 October, and the minimum aircraft-reported pressure was 1004 mb at 0600 UTC 8 October. Caravelle, Martinique, reported 39-kt sustained winds with a gust to 50 kt around 0600 UTC 8 October.

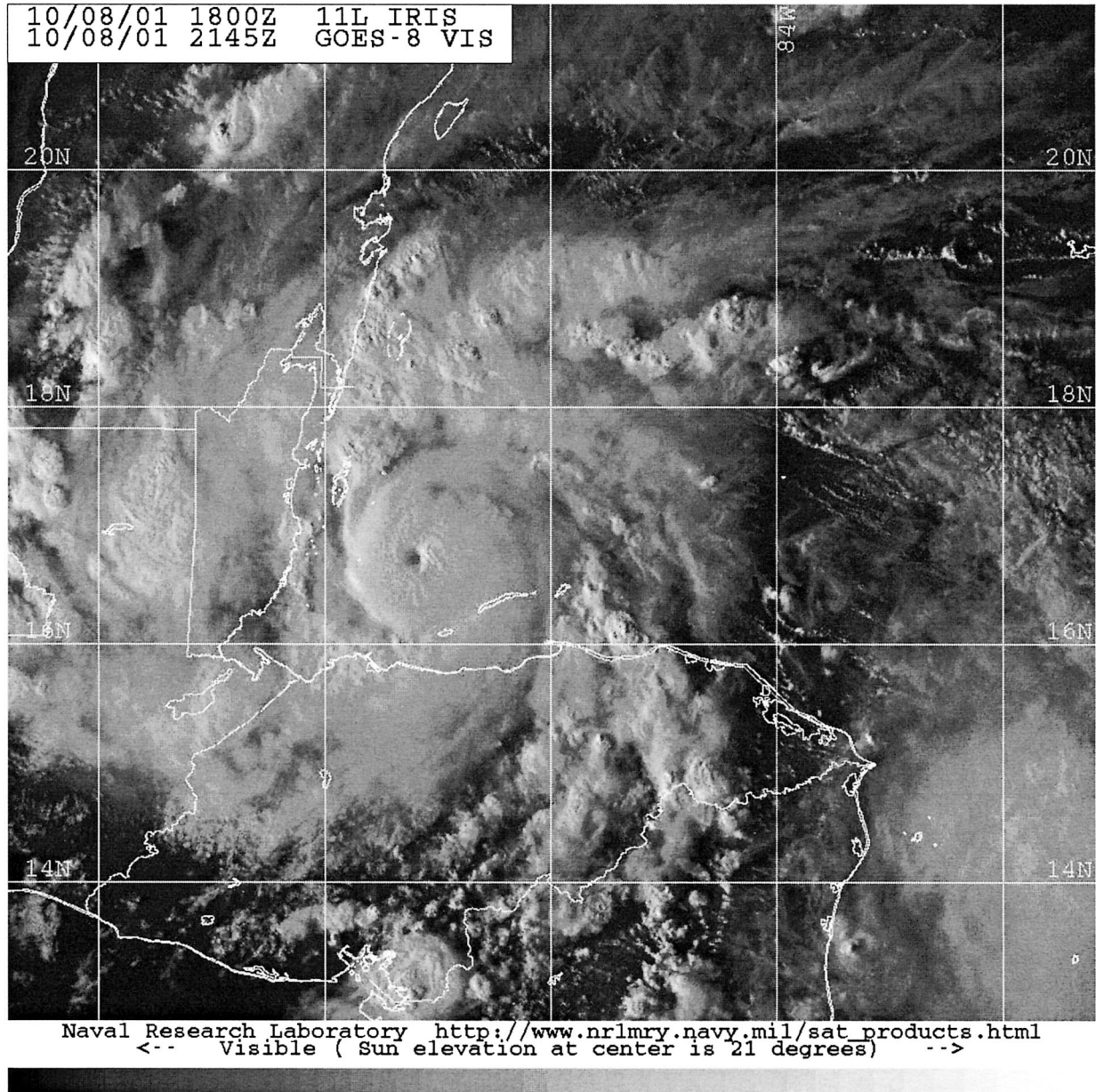


FIG. 5. GOES-8 visible image of Hurricane Iris nearing peak intensity at 2145 UTC 8 Oct 2001. Image provided by the Naval Research Laboratory's Marine Meteorology Division in Monterey, CA.

k. Hurricane Karen (Subtropical Storm One)

Karen was a category-1 hurricane of baroclinic origin. The cyclone passed just south of Bermuda as a powerful subtropical storm, causing hurricane force wind gusts and widespread damage on the island. Karen later made landfall in Nova Scotia as a weak tropical storm.

1) SYNOPTIC HISTORY

Karen originated from a frontal system that stalled southeast of Bermuda on 10 October. A strong upper-

level trough digging southeastward off the U.S. east coast caused baroclinic cyclogenesis on 11 October about 300 n mi southeast of Bermuda. The cyclone intensified and moved northward, then turned northwestward as it became vertically aligned. By 0000 UTC 12 October, the system, although still baroclinic in satellite appearance, had developed enough organized convection to become a subtropical storm about 30 n mi south of Bermuda (Fig. 6). The storm turned northward later that day with a continued gradual increase in organization.

Deep convection increased significantly early on 13

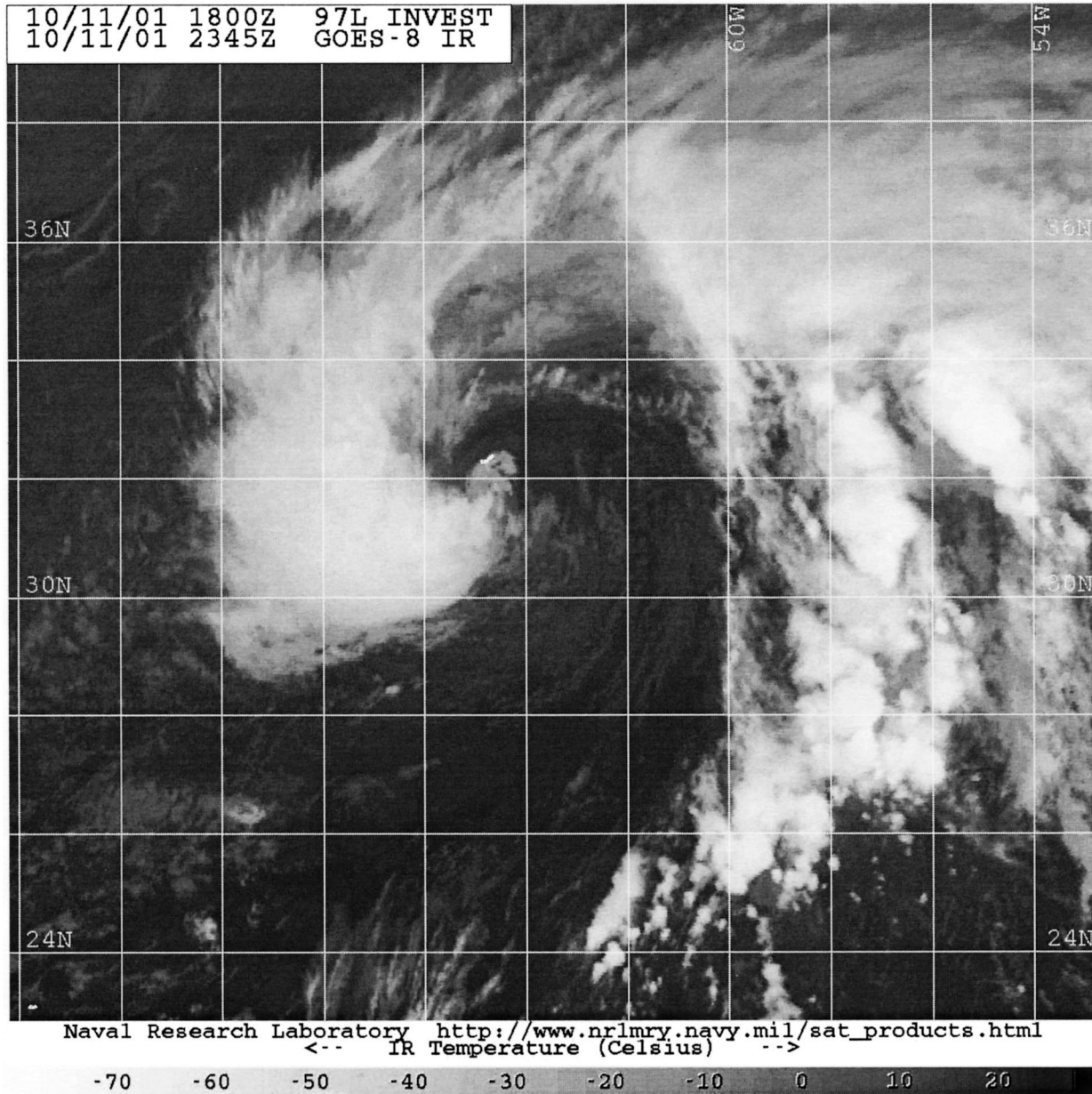


FIG. 6. GOES-8 infrared image of the subtropical storm that later became Hurricane Karen at 2345 UTC 11 Oct 2001. Image provided by the Naval Research Laboratory's Marine Meteorology Division in Monterey, CA.

October as the cyclone turned north-northeastward. By 0600 UTC that day, satellite microwave temperature data indicated the system had acquired a mid- to upper-level warm core. Based on this and the convective organization, the cyclone became a tropical storm at that time about 170 n mi north of Bermuda. Karen intensified slowly and became a hurricane 12 h later.

Karen turned northward and continued that general motion for the next 2 days. It reached its peak intensity of 70 kt early on 14 October about 350 n mi south of Halifax, Nova Scotia. Karen slowly weakened until it made landfall near Western Head, Nova Scotia, with

winds of 40 kt around 1200 UTC 15 October. The cyclone then turned northeastward and became extratropical again, before it was absorbed by a larger extratropical low located over the Gulf of St. Lawrence.

2) METEOROLOGICAL STATISTICS

The Bermuda airport reported sustained winds of 58 kt with gusts to 78 kt as Karen passed nearby during its subtropical storm phase. An anemometer at North Rock (91 m above sea level) reported 66-kt sustained winds with a gust to 85 kt. The cruise ship *Nordic Em-*

press (anchored in harbor at Bermuda) reported 79-kt sustained winds with a gust to 103 kt (47 m MSL) at 2317 UTC 11 October. The minimum pressure at the Bermuda airport was 992.0 mb, and the storm total rainfall was 68.6 mm. Cape George, Nova Scotia, reported sustained winds of 41 kt with gusts to 56 kt at 1630 UTC 15 October. McNabs Island, Nova Scotia, also reported a gust to 56 kt.

Some beneficial rainfall of 35–45 mm occurred across portions of drought-stricken Nova Scotia and New Brunswick. However, due to the rapid forward speed and weakening trend at landfall, most areas of Nova Scotia, New Brunswick, and Prince Edward Island generally received less than 13 mm of rainfall. The Cape Race area received up to 150 mm of rain in less than 12 h during the final extratropical stage.

Karen was transforming from an extratropical to a subtropical storm as it passed Bermuda. The satellite appearance of the storm at closest approach was rather nontropical—more resembling an occluded low with fronts (Fig. 6). However, some central convection existed, and the Bermuda observations gave evidence of a radius of maximum winds of about 40 n mi—more characteristic of a tropical cyclone. Additionally, the Bermuda sounding at 2300 UTC 11 October (not shown) indicated a vertical wind profile more characteristic of a warm-core TC; 74-kt winds were observed at 871 mb, with weakening and veering winds in the mid- and upper levels. While the sounding temperature profile was more characteristic of a cold-core cyclone, temperatures in the 300–700-mb layer warmed 4°–7°C over a 24-h period as the storm approached.

An Air Force Reserve reconnaissance aircraft flew into Karen from 1600 to 2100 UTC 12 October. Center penetrations at 1725 and 1910 UTC indicated a radius of maximum wind of about 80 n mi (more characteristic of a subtropical storm) with a weaker inner maximum at about 40 n mi—corresponding to the radius suggested by the earlier Bermuda data. The 850-mb flight-level winds were 53 and 67 kt, respectively, which suggested surface winds of approximately 42 and 54 kt, respectively, when using a 0.80 reduction factor (Franklin et al. 2000). Dropwindsondes released northwest and southeast of the center indicated wind speeds of 60–63 kt in the boundary layer decreasing to less than 45 kt near the surface. The aircraft also indicated the presence of a warm core at flight level.

3) CASUALTY AND DAMAGE STATISTICS

No deaths were reported from Karen. Strong winds caused considerable tree and powerline damage on Bermuda. At one point, more than 23 000 people were without power. Three cruise ships weathered the storm in St. George Harbor without receiving any significant damage. However, the winds caused the cruise ship *Norwegian Majesty* to become adrift in the harbor with one minor injury reported. A dozen or so smaller vessels

also broke loose from their moorings and either ran aground or sank.

4) WARNINGS

No TC watches or warnings were required for Hurricane Karen because it did not become a tropical system until after it passed northwest of Bermuda. However, the government of Bermuda issued extratropical gale warnings about 15 h before the closest approach of the center and storm warnings about 6 h before the closest approach. The government of Canada issued extratropical marine storm warnings at least 24 h in advance for Nova Scotia. The MPC and TAFB also issued marine gale and storm warnings for their respective Atlantic high seas forecast areas of responsibility more than 24 h before the development of the powerful pre-Karen extratropical low.

l. Tropical Storm Lorenzo

Like Karen, Lorenzo originated from a baroclinic system. In late October, a strong mid- to upper-level trough had remained quasi-stationary for several days to the west and southwest of the Azores Islands. A low-level circulation developed beneath the trough on 26 October. By 27 October, the system had acquired enough organized thunderstorm activity to be classified as a tropical depression about 750 n mi south-southwest of the western Azores. The depression moved slowly westward for 2 days, then turned northwestward and became a minimal tropical storm around 0000 UTC 30 October. Shortly thereafter, Lorenzo turned northward with some increase in forward speed. On 31 October, Lorenzo accelerated north-northeastward, eventually merging with a frontal system about 600 n mi west of the Azores.

m. Hurricane Michelle

Michelle was a classic late-season category-4 hurricane. It was the strongest hurricane to hit Cuba since 1952, and it left a trail of death and destruction from Central America to the Bahamas.

1) SYNOPTIC HISTORY

Michelle originated from a tropical wave that moved westward across the coast of Africa on 16 October. The wave showed little development over the Atlantic or the eastern Caribbean Sea. Showers accompanying the wave increased on 26 October over the western Caribbean Sea, and a broad low pressure area formed near the coast of Nicaragua the next day. A gradual increase in organization followed, and aircraft reports indicated that the system became a tropical depression near 1800 UTC 29 October along the coast of Nicaragua, between Puerto Cabezas and Bluefields.

The depression meandered over eastern Nicaragua for

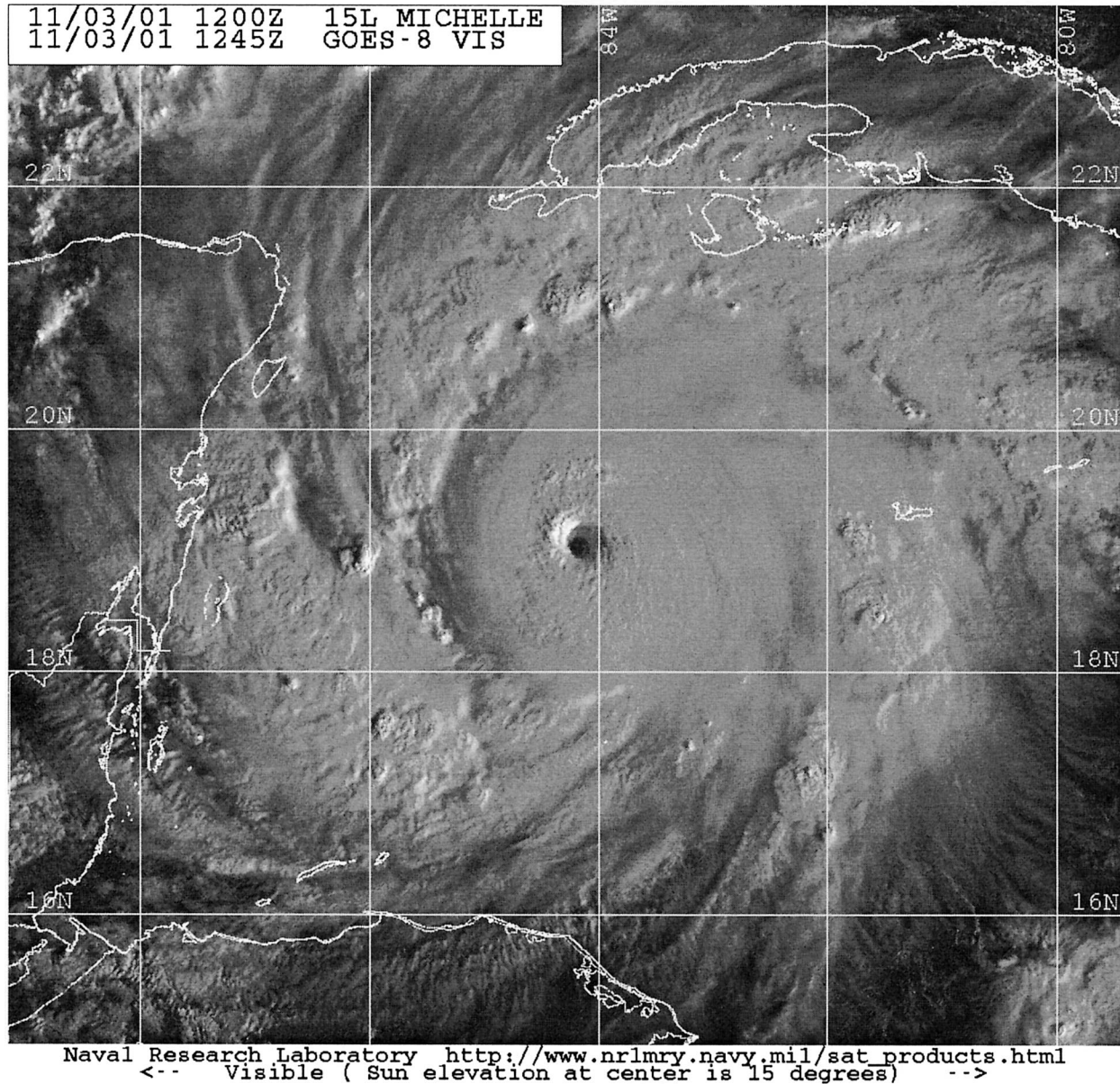


FIG. 7. GOES-8 visible image of Hurricane Michelle at 1245 UTC 3 Nov 2001. Image provided by the Naval Research Laboratory's Marine Meteorology Division in Monterey, CA.

the next 36 h. A slow north-northeastward motion that began early on 31 October brought the center back over the Caribbean later that day near the Honduras–Nicaragua border. The depression became Tropical Storm Michelle near 0000 UTC 1 November while centered about 50 n mi from northeastern Honduras. Michelle moved slowly north-northwestward on 1 November, then drifted northward the next day as it became a hurricane. Rapid intensification then occurred, with maximum sustained winds increasing from 70 kt at 1200 UTC 2 October to 115 kt at 1200 UTC 3 October. The

central pressure fell 51 mb from 988 mb at 0605 UTC 2 October to 937 mb at 1115 UTC 3 October. Satellite imagery near the latter time (Fig. 7) showed a classically organized hurricane with a well-defined eye embedded in a central dense overcast surrounded by outer banding.

Michelle turned slowly north-northeastward after 1200 UTC 3 October with some fluctuations in intensity. The peak intensity of 120 kt occurred from 0600 to 1800 UTC 4 October as the hurricane accelerated northeastward. This motion brought the center of Michelle to the southwestern offshore islands of Cuba near 1800 UTC

TABLE 5. Hurricane Michelle, selected surface observations, 29 Oct–5 Nov 2001.

Location	Min sea level pressure		Max surface wind speed			Storm surge (m) ^c	Storm tide (m) ^d	Total rain (mm)
	Time (UTC)/date	Pressure (mb)	Time (UTC) ^a /date	Sustained (kt) ^b	Gust (kt)			
Bahamas								
Abaco			1500 5 Nov	63				
Eleuthera			1500 5 Nov	59				
Freeport (MYGF)			1300 5 Nov	40	52			
Georgetown			1350 5 Nov	39	51			
Lee Stocking Island (NOAA) ^f	1600 5 Nov	989.8	1600 5 Nov	45	54			
Marsh Harbor	1800 5 Nov	995.6			72			
Nassau (MYNN)	1500 5 Nov	983.7	1800 5 Nov	48	89			321.1
New Providence						1.5–2.4		
Cayman Islands								
Cayman Brac			N/A 4 Nov		35			
Grand Cayman	0900 4 Nov	1001.3	1400 4 Nov	23	38			165.6
Cuba								
Aguada de Pasajeros ^f (78335)	0030 5 Nov	958.5	2300 4 Nov	65 ^g	95			
Bainoa (78340)	2045 4 Nov	996.1	2240 4 Nov	49 ^g	76			83.3
Batabano (78322)	1900 4 Nov	995.3	2310 4 Nov	45 ^g	54			64.3
Bauta (78376)	2030 4 Nov	999.1	2100 4 Nov	49 ^g	60			40.4
Camilo Cienfuegos	0510 5 Nov	987.4	0515 5 Nov	46	63			104.9
Casablanca (78325)	2110 4 Nov	993.4	2115 4 Nov	60 ^g	72			44.5
Cayo Largo (MUCL)	N/A 4 Nov	949.7	N/A 4 Nov	108	113		3.0	
Ciego de Avila (MUCA)			N/A 4 Nov	27	43			
Cienfuegos (78344)	0100 5 Nov	958.9	2300 4 Nov	65 ^g	91			
Colón (78332)	2300 4 Nov	980.9	1900 4 Nov	38 ^g	79			86.1
Cuba-Francia (78309)	1656 4 Nov	991.7	1332 5 Nov	54 ^g	71			103.9 ^h
Güines (78323)	2030 4 Nov	993.4	0125 5 Nov	44 ^g	64			23.6
Güira de Melena (78320)	2055 4 Nov	997.7	0050 5 Nov	32 ^g	56			78.5
Havana (MUHA)			0150 5 Nov	36	58			
Jagüey Grande (78331)	0000 5 Nov	992.8	2100 4 Nov	84	113			234.2
Jibaro (78341)	0400 5 Nov	995.5	0415 5 Nov	37 ^g	58			86.1
Jovellanos (78330)	0000 5 Nov	985.3	2300 4 Nov	37 ^g	54			164.8
La Fe (78321)	1500 4 Nov	991.6	1900 4 Nov	54 ^g	60			118.9 ^h
Melena del Sur (78375)	2100 4 Nov	994.8	2253 4 Nov	43 ^g	73			60.7
Nueva Gerona (78221)	1730 4 Nov	994.3	1630 4 Nov	50 ^g	65			
Playa Girón (78333)	2300 4 Nov	960.5	1900 4 Nov	62	105			129.5
Punta del Este (78324)	1700 4 Nov	981.4	1645 4 Nov	69 ^g	86			300.5
Sagua La Grande (78338)	0410 5 Nov	977.0	0200 5 Nov	49 ^g	81			56.9
Sancti Spiritus (78349)	0600 5 Nov	990.1	0430 5 Nov	49 ^g	65			75.4
Santiago Las Vegas (78373)	2040 4 Nov	997.8	2055 4 Nov	49 ^g	74			57.7
Santo Domingo (78326)	0300 5 Nov	962.8	0500 5 Nov	64 ^g	85			61.2
Tapaste (78374)	2050 4 Nov	995.5	2100 4 Nov	38 ^g	65			97.5
Topes de Collantes (78342)			0505 5 Nov	54 ^g	65			193.0
Trinidad (78337)	0400 5 Nov	991.3	0435 5 Nov	38 ^g	64			121.1
Unión de Reyes (78327)	0000 5 Nov	986.6	0030 5 Nov	46 ^g	81			116.1
Varadero (78328)			0000 5 Nov	46 ^g	81			101.1
Venezuela (78346)	0650 5 Nov	993.0	1632 4 Nov	30	52			46.0
Yabú (78343)	0455 5 Nov	963.7	0300 5 Nov	60 ^g	73			46.5
Nicaragua								
Puerto Cabezas	2100 30 Oct	1004.1						
United States (FL)								
Fort Lauderdale (KFLL)	1200 5 Nov	1004.2	1453 5 Nov	29	41			32.2
Key West (KEYW)	0701 5 Nov	1002.3	0438 5 Nov	32	41	0.5		65.0
Marathon (KMTH)	0953 5 Nov	1001.2	0153 5 Nov	28	37	0.4		45.5
Miami (KMIA)	0956 5 Nov	1003.3	1529 5 Nov	17	32			30.7
Miami Beach	1105 5 Nov	1001.2	0805 5 Nov	37	44			27.9
NW Florida Bay COMPS	0930 5 Nov	1000.7	0900 5 Nov	32	41			
Pompano Beach (KPMP)	1100 5 Nov	1004.0	1300 5 Nov	24	35			30.0
Tamiami (KTMB)	1000 5 Nov	1003.0	1300 5 Nov	17	26			34.8

TABLE 5. (Continued)

Location	Min sea level pressure		Max surface wind speed			Storm surge (m) ^c	Storm tide (m) ^d	Total rain (mm)
	Time (UTC)/date	Pressure (mb)	Time (UTC) ^a /date	Sustained (kt) ^b	Gust (kt)			
C-MAN stations								
Dry Tortugas, FL (DRYF1)	0800 5 Nov	1005.4	1810 4 Nov	35 ^g	45			
Fowey Rocks, FL (FWYF1)	1000 5 Nov	1002.4	1410 5 Nov	46 ^g	53			
Lake Worth, FL (LKWF1)	1100 5 Nov	1004.3	1230 5 Nov	34 ^g	42			
Long Key, FL (LONF1)	1000 5 Nov	1000.7	1020 5 Nov	35 ^g	43			
Molasses Reef, FL (MLRF1)	1200 5 Nov	1000.0	0650 5 Nov	41 ^g	50			
Sand Key, FL (SANF1)	0600 5 Nov	1001.0	0500 5 Nov	42	48			
Settlement Point, Bahamas (SPGF1)	2000 5 Nov	1002.8	1310 5 Nov	36 ^g	43			
Sombrero Key, FL (SMKF1)	0900 5 Nov	1001.4	0730 5 Nov	43 ^g	50			

^a Time/date is for sustained wind when both sustained and gust are listed.

^b Except as noted, sustained wind averaging periods for C-MAN and U.S. land-based ASOS reports are 2 min; buoy averaging periods are 8 min. Reports from Cuba are 1-min averages.

^c Storm surge is water height above normal astronomical tide level.

^d Storm tide is water height above National Geodetic Vertical Datum (1929 mean sea level).

^e Estimated.

^f Station disabled by storm—incomplete record.

^g 10-min average.

^h 3 Nov total.

that day as a category-4 hurricane on the SSHS, and to the Cuban mainland near the Bay of Pigs about 5 h later.

The eye of Michelle was disrupted by its passage over Cuba and increasing mid- to upper-level southwesterly flow. This contributed to the cyclone gradually losing tropical characteristics on 5 November. The center accelerated northeastward off the coast of Cuba near 0600 UTC, passed over Andros Island in the Bahamas near 1200 UTC, and over Eleuthera Island near 1800 UTC. Michelle became a vigorous extratropical cyclone around 0000 UTC 6 October, and the circulation center could be followed for another 18 h before it was absorbed into a strong frontal system.

2) METEOROLOGICAL STATISTICS

The Air Force Reserve Hurricane Hunters made 40 center “fixes” of Michelle, and NOAA aircraft made 11 fixes while the center was near Cuba. The maximum observed flight-level winds at 700 mb were 135 kt at 0258 UTC 4 November about 18 n mi south-southwest of the center. An eyewall dropsonde near 0408 UTC that day reported 160-kt winds at the 841-mb pressure level, which were the maximum winds observed in Michelle. The maximum surface wind reported by land stations was 108 kt with a gust to 113 kt at Cayo Largo, Cuba, at an unknown time on 4 November. A 113-kt gust was also measured at Jagüey Grande, Cuba, that day. Abaco Island in the Bahamas reported 63-kt sustained winds at 1500 UTC 5 November, while Nassau reported a gust to 89 kt. Unofficial observations relayed by amateur radio from elsewhere in the Bahamas indicated sustained winds of 70–80 kt. Sustained tropical storm force winds occurred over portions of the Florida Keys and southeastern Florida. Bermuda reported trop-

ical storm force gusts, but these may have been more related to the frontal system that absorbed Michelle than to the storm itself. Additional selected surface observations are included in Table 5.

The minimum pressure observed by reconnaissance aircraft was 933 mb at 1921 and 2101 UTC 3 November. The lowest pressure observed on land was 949.7 mb at Cayo Largo on 4 November. Nassau reported a 983.7-mb pressure at 1500 UTC 5 November as the center passed just to the south. Puerto Cabezas, Nicaragua, reported a 1004.1-mb pressure at 2100 UTC 30 October while Michelle meandered over eastern Nicaragua.

A notable aspect of Michelle was that the aircraft-reported winds and pressures appeared somewhat out of phase. Aircraft-reported winds at the time of the minimum pressure were roughly 10 kt lower than in the mission 6 h earlier during rapid intensification. The wind speed and pressure then both increased simultaneously over the next 9–12 h as Michelle reached its peak intensity. This relationship could be partly due to sampling issues, as no aircraft were in the storm during the last 6 h of the rapid intensification phase when Michelle appeared best organized in satellite imagery.

After Michelle became extratropical, aircraft winds from 700 mb were as high as 106 kt. This would normally support surface winds of 90–95 kt using the eyewall reduction factors of Franklin et al. (2000). However, no significant convection was occurring at that time. Thus, the best track intensity is a more conservative 75 kt based on reduction factors for nonconvective situations.

Several ships encountered Michelle, with two ships experiencing the core of the storm. The first was the *Scan Partner*, which reported winds rated 8/9 on the Beaufort scale (34–47 kt) and a 988-mb pressure at 0730

UTC 2 November just before the cyclone reached hurricane strength. The second was from a ship with the call sign ELWU7 (name unknown), which reported 60-kt winds and a 995.0-mb pressure at 1200 UTC 5 November. Additionally, a drifting buoy near Cat Island in the Bahamas reported a 986.7-mb pressure at 1900 UTC 5 November.

The highest reported storm surge was 3 m at Cayo Largo, which reportedly inundated the entire island. Above normal tides, and battering waves 4–5 m high, affected other areas along the coasts of western and central Cuba, causing extensive coastal floods. In the Bahamas, storm surges of 1.5–2.4 m were reported from New Providence Island, while storm surges of unknown magnitude affected Andros, Eleuthera, Cat Island, Exuma, and Abaco. Storm surge heights of 0.3–1.0 m occurred along portions of the southeastern Florida coast and in the Florida Keys. These surge values were part of a prolonged period of strong onshore winds and high tides that produced significant beach erosion along portions of the Florida east coast. Above normal tides and large battering waves also affected the southern and western shores of the Cayman Islands.

The initial slow movement of Michelle and its precursor disturbance contributed to widespread heavy rains over areas of Honduras, eastern Nicaragua, northern Costa Rica, and Jamaica. Ten-day storm totals on Jamaica were as high as 951 mm at Comfort Castle, and there were numerous other totals of over 380 mm. Heavy rains also occurred over portions of Cuba, the Bahamas, and the Cayman Islands. Nassau reported 321.1 mm, while Punta del Este on the Island of Youth reported 300.4 mm. Outer rainbands also affected southern Florida, where rainfall totals were generally 25–75 mm.

Two tornadoes were reported in southern Florida. An F1 tornado occurred near Belle Glade, and a waterspout moved onshore at Key Biscayne and became an F0 tornado.

3) CASUALTY AND DAMAGE STATISTICS

Press reports indicated 17 deaths from Michelle: 6 in Honduras, 5 in Cuba, 4 in Nicaragua, and 2 in Jamaica. The deaths in Honduras, Nicaragua, and Jamaica were due to severe floods caused by heavy rains.

Michelle was the strongest hurricane to hit Cuba since Hurricane Fox in October 1952. Reports from the government of Cuba indicate widespread damage over the central and western parts of the island, with the provinces of Matanzas, Villa Clara, and Cienfuegos the hardest hit. A total of 12 579 homes were destroyed, with 166 515 others damaged. Additional damage occurred to businesses and infrastructure. Severe damage was also reported to the sugar cane crop near the path of the storm. The total economic loss was estimated at \$1.866 billion.

Heavy rains in Honduras and Nicaragua caused widespread floods with more than 100 000 people forced

from their homes. The hardest hit area was the province of Gracias a Dios in the northeastern part of Honduras. The northeastern part of Nicaragua near Puerto Cabezas was also hit by severe floods. Floods were also reported in portions of northern Costa Rica where several thousand people evacuated.

Flash floods and mudslides in Jamaica caused property damage. High surf and tides caused about \$28 million in damage in the Cayman Islands, primarily along the west coast of Grand Cayman. The two tornadoes in Florida were responsible for about \$20,000 in damage.

Additionally, a NOAA P-3 aircraft returned from a flight into Michelle with damage to the tail section, wings, and propellers.

4) WARNINGS

The intensity and generally well-forecast motion of Michelle produced long lead times for watches and warnings in Cuba. Hurricane watches were issued 51 h before the center reached the coastal islands of Cuba, while hurricane warnings were issued 31 h before the center arrived. The warnings and the long lead times allowed 600 000 people to be evacuated from the threatened portions of the island. In the Bahamas, hurricane watches were issued 33 h before the center reached Andros Island, while hurricane warnings were issued 21 h before the center arrived. In the Florida Keys, a tropical storm warning and a hurricane watch were issued about 42–48 h before the arrival of the worst conditions, and a hurricane warning was issued 18–24 h before the worst conditions. Tropical storm warnings were somewhat short-fused in the Cayman Islands, where they were issued about 6–12 h before the closest approach of the center. This was due mainly to a somewhat earlier than expected northeastward turn. However, a tropical storm watch was issued for Grand Cayman Island about 42 h before the closest approach of the center.

n. Hurricane Noel

Noel developed from yet another nontropical low over the east-central Atlantic. The low formed late on 1 November near 32°N, 42°W. It deepened and occluded as it moved slowly west-northwestward over the next 48 h. The low gradually developed organized convection, and it is estimated that it became a subtropical storm 775 n mi south of Cape Race around 0000 UTC 4 November (Fig. 1). The storm turned northward with its forward speed increasing to about 10 kt late that day. Convection became more symmetric and formed a 120 n mi wide ring around the center early on 5 November. Microwave sounding data indicated that the system developed a weak midlevel warm core by 1200 UTC that day. This, along with a report of 65 kt and 992.0 mb from the ship *Tellus* at 1400 UTC, indicated that the cyclone had become a hurricane about 535 n mi south-

southeast of Cape Race. Vertical shear caused Noel to weaken to a tropical storm early on 6 November. It then accelerated northward and became extratropical about 285 n mi southeast of Cape Race. The extratropical low was absorbed by a larger extratropical system later that day.

o. Hurricane Olga (Subtropical Storm Two)

Olga was the last in a succession of nontropical systems in the east-central Atlantic that tried and/or succeeded in becoming TCs during October and November. Surface observations and satellite imagery showed pressure falls and increasing disturbed weather between Bermuda and the Leeward Islands as early as 21 November. A cold front reached the area on 22 November, aiding in the formation of an extratropical low. The low intensified and developed organized convection, and it is estimated that it became a subtropical storm at 0000 UTC 24 November about 780 n mi east-southeast of Bermuda (Fig. 1). Convection continued to become concentrated near the center and it is estimated that by 1200 UTC that day the core of the cyclone had acquired enough tropical characteristics to be considered a tropical storm. However, the cyclone still had some nontropical characteristics as it remained embedded within a much larger extratropical circulation.

Olga moved northeastward on 24 November, followed by westward and southwestward turns the next day. This was followed by a double loop from 26 to 28 November. Olga reached hurricane strength on 26 November and its maximum intensity of 80 kt the next day. After the second loop, Olga turned southwestward on 29 November and encountered increasing vertical shear. It weakened to a tropical storm that day and to a tropical depression on 30 November. As Olga turned north-northwestward on 1 December shear decreased, which allowed the cyclone to regain tropical storm strength the next day. Olga continued north-northwestward until 3 December, when it turned eastward. The system weakened to a depression on 4 December as it turned southeastward. It became a trough later that day about 600 n mi east of Nassau. The remnants of Olga subsequently moved westward into the Gulf of Mexico bringing gusty winds and locally heavy rains to portions of the Bahamas, Cuba, and southern Florida.

Ship reports played an important role in tracking Olga. The most significant observation came from the German sailing yacht *Manana Tres* (call sign unknown), which reported a pressure of 989 mb near the center at 0900 UTC 24 November. The ship *Liberty Sun* (call sign WCOB) encountered the center of Olga during 25–26 November, reporting 55-kt winds at 1800 UTC 25 November and a 981.4-mb pressure 6 h later. Large swells from Olga affected the islands of the northeastern Caribbean, the Bahamas, and the east coast of the United States. The only known damage, however, was to the *Manana Tres*.

3. Other tropical weather systems

a. Tropical depressions

In addition to the named TCs described above, there were two tropical depressions that did not reach tropical storm strength.

Tropical Depression Two formed from a tropical wave about 1000 n mi east of the Windward Islands on 11 July. The system moved rapidly westward and weakened back to a tropical wave late the next day due to vertical wind shear. The wave moved through the Lesser Antilles on 13–14 July, producing some showers.

Tropical Depression Nine formed over the southwestern Caribbean Sea on 19 September from a tropical wave that emerged from the coast of Africa on 11 September. Upper-level conditions appeared favorable for development, but the cyclone moved into eastern Nicaragua early on 20 September before it could become a tropical storm. Although the depression dissipated over land later that day, the tropical wave continued across Central America into the Pacific where it spawned Hurricane Juliette (Avila et al. 2003).

b. Tropical waves

Tropical waves play a dominant role in the development of tropical cyclones in the Atlantic and in the eastern North Pacific Oceans along with being responsible for modulation of rainfall in the Caribbean basin. Avila et al. (2000) describe the methodology the NHC uses to track tropical waves from Africa across the tropical Atlantic, the Caribbean Sea, and Central America into the Pacific. During the May–November 2001 period, 64 tropical waves were tracked from the west coast of Africa to the Caribbean. This is slightly above the 1967–2000 average number of waves, which is about 60. Most of them continued into the eastern North Pacific basin where they provided the initial disturbances for all 15 named tropical cyclones in 2001 (Avila et al. 2003).

In 2001, 9 out of 63 waves (14%) spawned Atlantic tropical cyclones. This compares to the average of 10% of these waves developing into Atlantic tropical storms or hurricanes (Avila et al. 2000). Nine of the named tropical cyclones (60%) in 2001, including all four major hurricanes, formed from tropical waves, which is near the 63% average observed from 1967 to 2000. However, this percentage is lower than that observed during 2000 (71%), and much lower than that observed in 1998 (86%) and 1999 (91%) (Franklin et al. 2001).

Examples of tropical wave structure can be seen in the time–height section for Guadeloupe for the month of August in Fig. 8 and in a sequence of twice-a-day infrared satellite images from 16 to 22 August displayed in Fig. 9. This sample is representative of the synoptic pattern prevailing during the season. It shows a cyclonic wind shift every 3 or 4 days as a wave passed over that station. The wind shift, in some waves, was more pro-

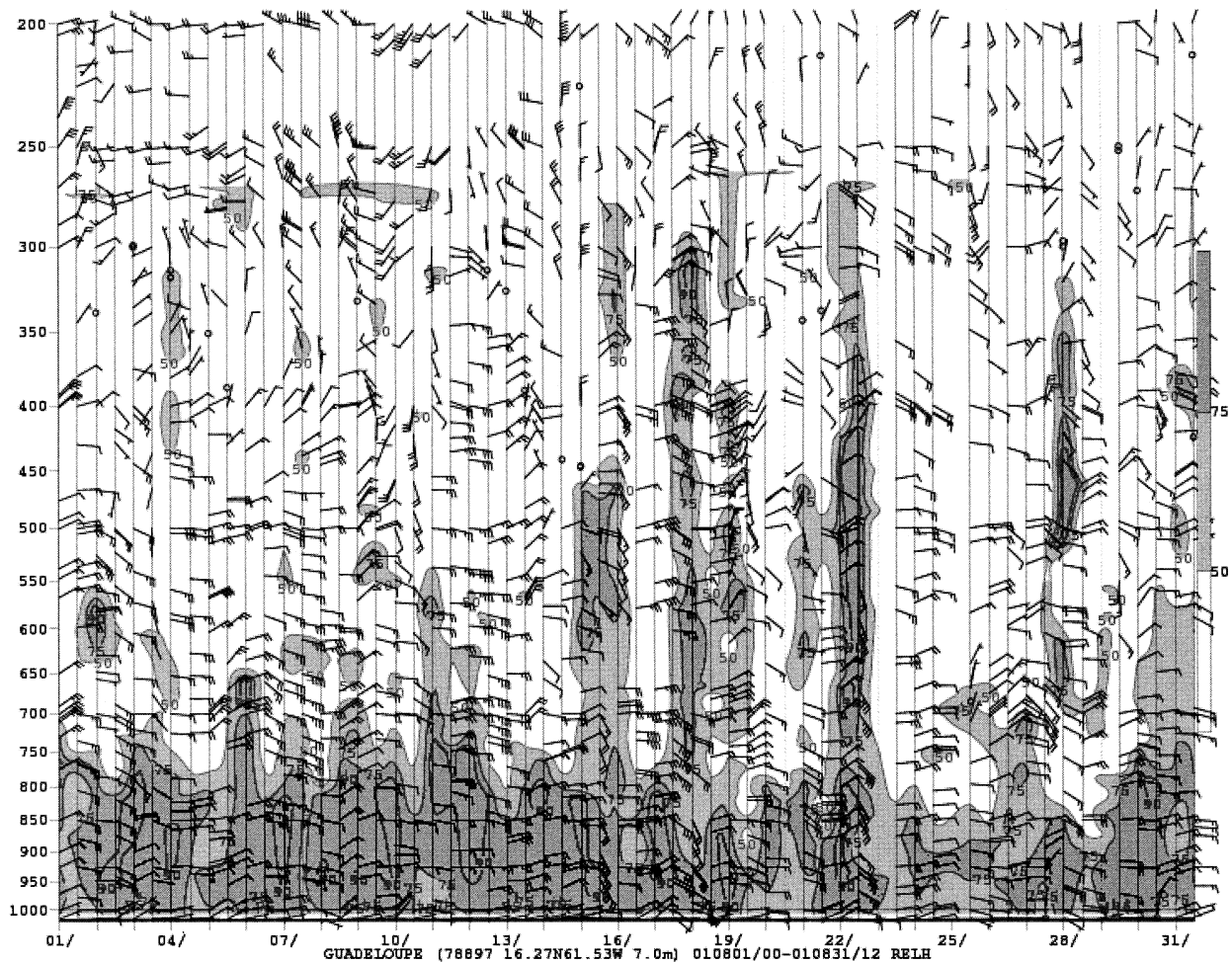


FIG. 8. Vertical time section of wind and relative humidity at Guadeloupe from 1 to 30 Aug 2001. Wind plotted every 12 h according to convection with each full and half barb denoting 10 and 5 kt, respectively, and the solid flag denoting 50 kt. Relative humidity contours at 50%, 75%, and 90%. Relative humidity shading at 50% and 75%.

nounced near the 700-mb level and extended to near 300 mb. The time–height section also shows columns of high relative humidity accompanying the waves. These waves caused clusters of shower activity to emerge periodically from the west coast of Africa and move westward across the Atlantic basin as shown in Fig. 9. However, not all waves are convectively active and some others have already triggered a tropical cyclone during this period. For example, note the tropical wave associated with Chantal moving over the Caribbean Sea from 16 to 20 August and the wave that triggered Dean crossing the Lesser Antilles on 20 August.

A comparison of the tropical waves in 2001 with other seasons shows little annual variation in the structure of tropical waves. However, the number of tropical cyclones forming from tropical waves varies annually. This variation is mostly related to the prevailing large-scale environment and not to the waves. For example, in years when strong vertical wind shear prevails in the deep Tropics or the atmosphere is more stable than nor-

mal, the number of tropical storms and hurricanes developing from waves is small despite formation of a nearly climatological number of waves.

4. Forecast verification

Every 6 h, the National Hurricane Center issues an advisory “package” for all TCs in the Atlantic (and northeastern Pacific) basin(s). This package includes 12-, 24-, 36-, 48-, and 72-h official forecasts of the TC center location and maximum 1-min wind speed (at a 10-m elevation) associated with the cyclone circulation. These forecasts are verified by comparison with best track positions and wind speeds described earlier. A track forecast error is defined as the great-circle distance between a forecast center location and a best track position for the same time. A wind speed forecast error is the absolute value of the difference between a forecast wind speed and best track wind speed.

Table 6 lists the official average track forecast errors

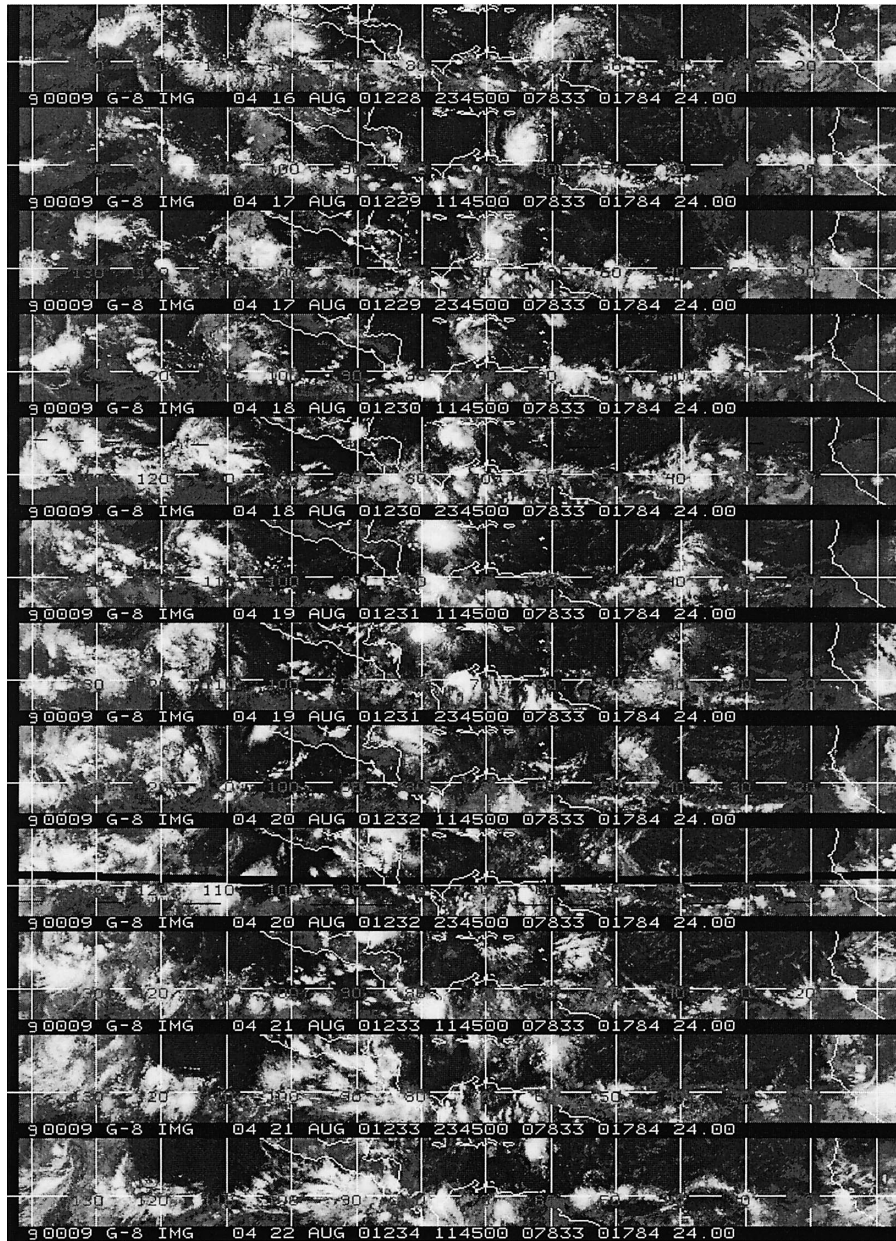


FIG. 9. Time sequence of GOES infrared images (Hovmöller diagram) taken twice a day at 1145 and 2345 UTC from 16 to 22 Aug 2001. The latitude belt is roughly 5°–20°N.

for the 2001 season and the average error for the previous 10-yr period. Also listed are the climatology and persistence (CLIPER) model track errors. The CLIPER model is a simple statistical model derived from the best tracks of past TCs (Aberson 1998); it represents a “no skill” accuracy level.

The 2001 average official track errors are small—5%–17% less than the 1991–2000 average and 26%–51% less than the corresponding CLIPER errors. Moreover, the 2001 average errors for 36, 48, and 72 h are the lowest yearly averages since records began. In contrast, the 2001 CLIPER errors were 9%–12% larger than

the 1991–2000 CLIPER errors, indicating that forecasts in 2001 were more difficult than usual. The small official track forecast errors continue an improvement trend reported by McAdie and Lawrence (2000) and can be attributed to improved numerical guidance. The 2001 official track errors were also more skillful than the previous 10 yr, as the 1991–2000 official errors were only 15%–35% smaller than the 1991–2000 CLIPER errors.

The track forecasts for Hurricane Michelle are particularly noteworthy. The average official errors were 30, 52, 75, 96, and 126 n mi at 12, 24, 36, 48, and 72 h,

TABLE 6. Official and CLIPER track forecast errors in the Atlantic basin for the 2001 season and for the period 1991–2000.

	Forecast period (h)				
	12	24	36	48	72
2001 avg official error (n mi)	42	74	100	125	188
2001 avg CLIPER error (n mi)	57	123	187	253	375
2001 avg official error relative to CLIPER	-0.26	-0.40	-0.47	-0.51	-0.50
2001 no. of cases	217	182	153	133	99
1991–2000 avg official error (n mi)	44	82	118	150	226
1991–2000 avg CLIPER error (n mi)	52	110	172	232	343
1991–2000 avg official error relative to CLIPER	-0.15	-0.25	-0.31	-0.35	-0.34
1991–2000 no. of cases	2049	1835	1646	1475	1187
2001 official error relative to 1991–2000 official	-0.05	-0.10	-0.15	-0.17	-0.17
2001 CLIPER error relative to 1991–2000 CLIPER	0.10	0.12	0.09	0.09	0.09

respectively. These errors are 30%–40% better than the 1991–2000 average for 12–48 h and 40%–50% better than the 1991–2000 average at 72 h. They are also 20%–30% better than CLIPER at 12 and 24 h and 30%–40% better at other times. As excellent as the official forecasts were, forecasts from the Aviation Model run of the National Weather Service's Medium-Range Forecast model were even better. The average errors for the model and the interpolated previous model run used in official forecasts were 58 n mi or less for all the forecast times—an excellent set of forecast errors.

Table 7 lists the official average wind speed forecast errors for this season and for the previous 10 yr. The Statistical Hurricane Intensity Forecast (SHIFOR) model intensity errors are also listed. SHIFOR (Jarvinen and Neumann 1979) is a statistical wind speed forecast model and is the analog to CLIPER for determining the skill of a wind speed forecast.

The 2001 official wind speed errors were nearly the same as the previous 10-yr averages at all forecast periods except 72 h, where the average was 25% smaller. However, the 2001 intensity forecasts were skillful in that the official errors ranged from 11% to 28% less than the 2001 SHIFOR errors.

5. Discussion

Most of the 2001 season's activity occurred in the subtropics and no TC reached hurricane strength in the

area south of 23°N and east of 70°W. This was a significant anomaly, as during the less or equally active 1998–2000 hurricane seasons four cyclones in each season became hurricanes in this area. NHC records show that this was the first time since 1993 that no TCs reached hurricane strength in this region, and that no other season (since 1871) had 15 or more tropical storms without a hurricane developing in this region. It is notable that the lack of hurricanes in the region was *not* due to lack of candidates; six tropical storms and a tropical depression formed in this area in 2001.

Another aspect of the season was the role of baroclinic energetics in the genesis and development of cyclones as defined by Kimberlain (1996). Gabrielle, Karen, Lorenzo, Noel, and Olga all formed from nontropical weather systems, with Karen showing a classic subtropical storm evolution (Hebert and Potat 1975). Humberto formed on a trough trailing from Gabrielle that developed as the latter cyclone became extratropical. Gabrielle itself interacted with a frontal system, which gave it a structure more resembling a hybrid storm (Beven 1997) even at hurricane strength. Allison's genesis was influenced by an upper-level low, and later interaction with an upper-level trough caused the cyclone to become subtropical for much of its life cycle. In addition to the named storms, three other nontropical systems in the central and eastern Atlantic almost became tropical or subtropical cyclones during October and November.

TABLE 7. Official and SHIFOR intensity forecast errors in the Atlantic basin for the 2001 season and for the period 1991–2000.

	Forecast period (h)				
	12	24	36	48	72
2001 avg official error (kt)	6.3	10.5	13.3	15.9	14.7
2001 avg SHIFOR error (kt)	8.7	12.9	15.9	17.8	16.8
2001 avg official error relative to SHIFOR	-0.28	-0.19	-0.16	-0.11	-0.13
2001 no. of cases	215	181	152	133	99
1991–2000 avg official error (kt)	7.0	10.8	13.7	16.3	19.6
1991–2000 avg SHIFOR error (kt)	8.6	12.6	15.6	18.2	20.8
1991–2000 avg official error relative to SHIFOR	-0.19	-0.14	-0.12	-0.10	-0.06
1991–2000 no. of cases	2045	1829	1644	1470	1186
2001 official error relative to 1991–2000 official	-0.10	-0.03	-0.03	-0.02	-0.25
2001 SHIFOR error relative to 1991–2000 SHIFOR	0.01	0.02	0.02	-0.02	-0.19

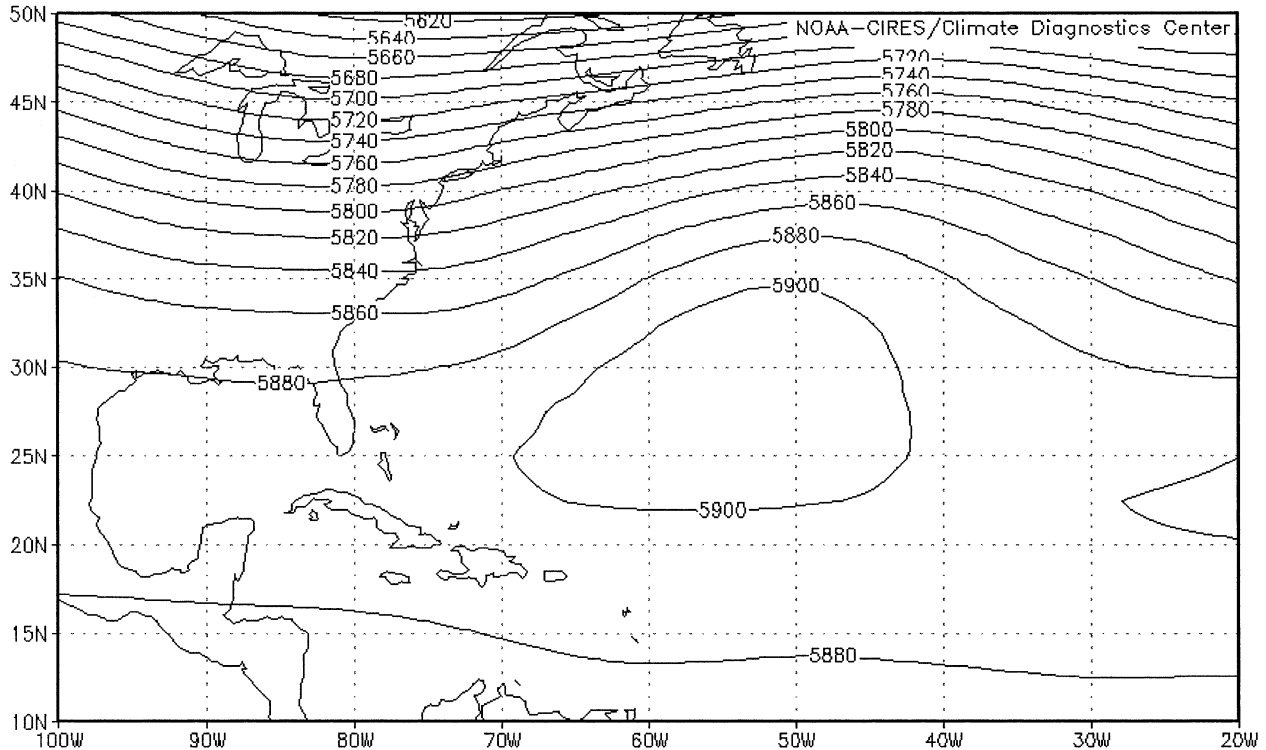


FIG. 10. Mean 500-mb heights (gpm) for Aug–Oct 2001. Height data provided by the NOAA–CIRES Climate Diagnostics Center, Boulder, CO (see their Web site for more information: <http://www.cdc.noaa.gov/>). Contour interval is 20 gpm.

A similar, though less pronounced, baroclinic influence was seen in the 2000 season, where three cyclones formed from nontropical systems and two others showed significant baroclinic influence during development. These seasons stand in sharp contrast to the 1999 season, when only one system had a nontropical origin. Such season-to-season variability has been documented before (Kimberlain and Elsner 1998).

A third aspect was the lack of hurricane landfalls in the United States. This made the 2001 season the fourth season (after 1951, 1990, and 2000) to have eight or more hurricanes and not have a landfall on the U.S. mainland. Part of the explanation for the lack of U.S. landfalls is found in mean August–October 500-mb geopotential height fields (Fig. 10). The figure shows a mean anticyclone in the Atlantic centered near 27°N, 54°W, with a ridge extending westward along 24°–25°N all the way to Mexico and a second ridge extending east-southeastward. A broad trough was present over the eastern United States. Comparison with Fig. 1 indicates three storms that formed during this period (Chantal, Iris, and Jerry) were south of the ridge axis and moved generally westward. Five other storms (Barry, Gabrielle, Humberto, Karen, and Lorenzo) formed north of the mean ridge axis and were mostly steered away from the United States. The pattern suggests that it would be difficult for the 2001 cyclones to hit the United States during the August–October period, with

Barry and Gabrielle forming in the Gulf of Mexico having the best chance to do so. Chance played a role as well. Both Barry and Gabrielle were near hurricane strength at landfall, and only slight changes in vertical shear or time of landfall would have allowed both systems to become hurricanes.

One significant similarity of 2001 to the active hurricane seasons since 1995 was the development of a late-season (October–November) hurricane in the western Caribbean Sea. The TPC records indicate that Michelle was the eighth such hurricane during the period 1995–2001. This contrasts sharply with the period 1982–94, when no late-season hurricanes occurred in this area.

Acknowledgments. The authors wish to thank the Naval Research Laboratory's tropical cyclone Web page team headed by Jeff Hawkins and the National Climatic Data Center in Asheville, North Carolina, for the satellite imagery. Stephen R. Baig produced the track chart, while Jim Gross produced the forecast verification statistics. The NOAA/Climate Diagnostics Center provided the mean 500-mb geopotential heights. The meteorological services of the Bahamas, Belize, the Cayman Islands, Cuba, Jamaica, Mexico, Nicaragua, and the various islands of the Lesser Antilles provided the meteorological data for those countries.

REFERENCES

- Aberson, S. D., 1998: Five-day tropical cyclone track forecasts in the North Atlantic basin. *Wea. Forecasting*, **13**, 1005–1015.
- , and J. L. Franklin, 1999: Impact on hurricane track and intensity forecasts of GPS dropwindsonde observations from the first season flights of the NOAA Gulfstream-IV jet aircraft. *Bull. Amer. Meteor. Soc.*, **80**, 421–427.
- Avila, L. A., R. J. Pasch, and J. Jiing, 2000: Atlantic tropical systems of 1996 and 1997: Years of contrasts. *Mon. Wea. Rev.*, **128**, 3695–3706.
- , —, J. L. Beven, J. L. Franklin, M. B. Lawrence, S. R. Stewart, and J. Jiing, 2003: Eastern North Pacific hurricane season of 2001. *Mon. Wea. Rev.*, **131**, 249–262.
- Beven, J. L., 1997: A study of three “hybrid” storms. Preprints, *22d Conf. on Hurricanes and Tropical Meteorology*, Fort Collins, CO, Amer. Meteor. Soc., 645–646.
- Brueske, K. F., C. S. Velden, B. W. Kabat, and J. D. Hawkins, 2002: Tropical cyclone intensity estimation using the NOAA-KLM Advanced Microwave Sounding Unit (AMSU): Part 1—Initial field test and lessons learned. Preprints, *25th Conf. on Hurricanes and Tropical Meteorology*, San Diego, CA, Amer. Meteor. Soc., 481–482.
- Dvorak, V. F., 1984: Tropical cyclone intensity analysis using satellite data. NOAA Tech. Rep. NESDIS 11, 47 pp.
- Franklin, J. L., L. A. Avila, M. L. Black, and K. Valde, 2000: Eyewall wind profiles in hurricanes determined by GPS dropwindsondes. Preprints, *24th Conf. on Hurricanes and Tropical Meteorology*, Fort Lauderdale, FL, Amer. Meteor. Soc., 446–447.
- , —, J. L. Beven, M. B. Lawrence, R. J. Pasch, and S. R. Stewart, 2001: Atlantic hurricane season of 2000. *Mon. Wea. Rev.*, **129**, 3037–3056.
- Hawkins, J. D., T. F. Lee, J. Turk, C. Sampson, F. J. Kent, and K. Richardson, 2001: Real-time Internet distribution of satellite products for tropical cyclone reconnaissance. *Bull. Amer. Meteor. Soc.*, **82**, 567–578.
- Hebert, P. J., 1973: Subtropical cyclones. *Mar. Wea. Log*, **17**, 203–207.
- , and K. O. Poteat, 1975: A satellite classification technique for subtropical cyclones. NOAA Tech. Memo. NWS SR-83, 25 pp. [Available from National Weather Service, Fort Worth, TX 76102.]
- Hock, T. F., and J. L. Franklin, 1999: The NCAR GPS dropwindsonde. *Bull. Amer. Meteor. Soc.*, **80**, 407–420.
- Jarvinen, B. R., and C. J. Neumann, 1979: Statistical forecasts of tropical cyclone intensity for the North Atlantic basin. NOAA Tech. Memo. NWS NHC-10, 22 pp.
- Kimberlain, T. B., 1996: Baroclinically-initiated hurricanes of the North Atlantic basin. M.S. thesis, Dept. of Meteorology, The Florida State University, 204 pp. [Available from Department of Meteorology, The Florida State University, Tallahassee, FL 32306-3034.]
- , and J. B. Elsner, 1998: The 1995 and 1996 North Atlantic hurricane seasons: A return to the tropical-only hurricane. *J. Climate*, **11**, 2062–2069.
- Mainelli, M., M. DeMaria, and L. K. Shay, 2002: The impact of oceanic heat content on hurricane forecasting using SHIPS. Preprints, *25th Conf. on Hurricanes and Tropical Meteorology*, San Diego, CA, Amer. Meteor. Soc., 627–628.
- McAdie, C. J., and M. B. Lawrence, 2000: Improvements in tropical cyclone track forecasting in the Atlantic basin, 1970–98. *Bull. Amer. Meteor. Soc.*, **81**, 989–997.
- Nieman, S. J., W. P. Menzel, C. M. Hayden, D. Gray, S. T. Wanzong, C. S. Velden, and J. Daniels, 1997: Fully automated cloud-drift winds in NESDIS operations. *Bull. Amer. Meteor. Soc.*, **78**, 1121–1133.
- Simpson, R. H., 1974: The hurricane disaster potential scale. *Weatherwise*, **27**, 169, 186.
- Tsai, W.-Y., M. Spender, C. Wu, C. Winn, and K. Kellogg, 2000: SeaWinds of QuikSCAT: Sensor description and mission overview. *Proc. Geoscience and Remote Sensing Symp. 2000*, Vol. 3, Honolulu, HI, IEEE, 1021–1023.